

1 **Phytochemical Nrf2 activator attenuates skeletal muscle mitochondrial dysfunction and**  
2 **impaired proteostasis in a preclinical model of musculoskeletal aging**

7 Robert V. Musci<sup>1\*</sup>, Kendra M. Andrie<sup>3#</sup>, Maureen A. Walsh<sup>1</sup>, Zackary J. Valenti<sup>1</sup>, Maryam F.  
8 Afzali<sup>3</sup>, Taylor Johnson<sup>1</sup>, Thomas E. Kail<sup>1</sup>, Richard Martinez<sup>3</sup>, Tessa Nguyen<sup>1</sup>, Joseph L.  
9 Sanford<sup>1,3</sup>, Meredith D. Murrell<sup>4</sup>, Joe M. McCord<sup>5,6</sup>, Brooks M. Hybertson<sup>5,6</sup>, Benjamin F. Miller<sup>7</sup>,  
10 Qian Zhang<sup>1</sup>, Martin A. Javors<sup>4</sup>, Kelly S. Santangelo<sup>3</sup>, Karyn L. Hamilton<sup>1,2</sup>

11  
12  
13 <sup>1</sup>Department of Health and Exercise Science, Colorado State University, Fort Collins, CO, USA  
14 <sup>2</sup>Columbine Health Systems Center for Healthy Aging, Colorado State University, Fort Collins,  
15 CO, USA

16 <sup>3</sup>Department of Microbiology, Immunology, and Pathology, Colorado State University, Fort  
17 Collins, CO, USA

18 <sup>4</sup>Department of Psychiatry, UT Health San Antonio, TX, USA

19 <sup>5</sup>Pathways Bioscience, Aurora, CO

20 <sup>6</sup>Department of Medicine, Division of Pulmonary Sciences and Critical Care Medicine, University  
21 of Colorado Anschutz Medical Campus, Aurora, CO

22 <sup>7</sup>Aging and Metabolism Research Program, Oklahoma Medical Research Foundation,  
23 Oklahoma City, OK, USA.

24

25 \* Correspondence:

26 Robert V. Musci

27 [rmusci@genetics.utah.edu](mailto:rmusci@genetics.utah.edu)

28

29 # Current affiliation:

30 Unit for Laboratory Animal Medicine, University of Michigan Medical School, Ann Arbor, MI,  
31 USA

32

33 **Abstract:** Musculoskeletal dysfunction is an age-related syndrome associated with impaired  
34 mitochondrial function and proteostasis. However, few interventions have tested targeting two  
35 drivers of musculoskeletal decline. Nuclear factor erythroid 2-related factor 2 (Nrf2) is a  
36 transcription factor that stimulates transcription of cytoprotective genes and improves  
37 mitochondrial function. We hypothesized daily treatment with a Nrf2 activator in Hartley guinea  
38 pigs, a model of age-related musculoskeletal dysfunction, attenuates the progression of skeletal  
39 muscle mitochondrial dysfunction and impaired proteostasis, preserving musculoskeletal  
40 function. We treated 2-month- and 5-month-old male and female Hartley guinea pigs for 3 and  
41 10 months, respectively, with the phytochemical Nrf2 activator PB125 (Nrf2a). Longitudinal  
42 assessments of voluntary mobility were measured using Any-Maze™ open-field enclosure  
43 monitoring. Cumulative skeletal muscle protein synthesis rates were measured using deuterium  
44 oxide over the final 30 days of treatment. Mitochondrial oxygen consumption in permeabilized  
45 soleus muscles was measured using *ex vivo* high resolution respirometry. In both sexes, Nrf2a  
46 1) increased electron transfer system capacity; 2) attenuated the disease/age-related decline in  
47 coupled and uncoupled mitochondrial respiration; and 3) attenuated declines in protein  
48 synthesis in the myofibrillar, mitochondrial, and cytosolic subfractions of the soleus. These  
49 improvements were not associated with statistically significant prolonged maintenance of  
50 voluntary mobility in guinea pigs. Collectively, these results demonstrate that treatment with an  
51 oral Nrf2 activator contributes to maintenance of skeletal muscle mitochondrial function and  
52 proteostasis in a pre-clinical model of musculoskeletal decline. Further investigation is  
53 necessary to determine if these improvements are also accompanied by slowed progression of  
54 other aspects of musculoskeletal decline.

55

56 249/250 words

57

58 **keywords:** proteostasis, mitochondria, skeletal muscle, musculoskeletal, chronic disease,  
59 ageing, healthspan, lifespan, longevity

60 **Introduction**

61 Targeting the age-related processes that underpin chronic diseases to promote “healthy  
62 longevity” or extend the healthspan (Kaeberlein *et al.*, 2015) is essential to decrease both  
63 healthcare (Atella *et al.*, 2019) and financial (Goldman *et al.*, 2013) burdens imposed by an  
64 increasingly aged population. Moreover, preserving health at later ages would allow for  
65 individuals to maintain a greater quality of life. There is a growing list of interventions (Bakula *et*  
66 *al.*, 2019) that target the hallmarks (Lopez-Otin *et al.*, 2013) and pillars (Kennedy *et al.*, 2014) of  
67 aging. Thus, evaluating these interventions in translational pre-clinical models represents an  
68 essential next-step in developing therapeutics for the human population.

69 The musculoskeletal system is comprised of bones, joints, cartilage, tendon, and  
70 skeletal muscle, all of which are physically and biochemically connected (Bonewald *et al.*, 2013;  
71 DiGirolamo *et al.*, 2013). Age-related decline in musculoskeletal function contributes to the  
72 health burden associated with aging (Goates *et al.*, 2019). Musculoskeletal dysfunction imparts  
73 a loss of mobility and independence (Roux *et al.*, 2005) and leads to frailty (Walston *et al.*,  
74 2006). It also exacerbates comorbidities including cardiometabolic disease (Baskin *et al.*, 2015),  
75 cancer (Williams *et al.*, 2018), and cognitive decline (Ogawa *et al.*, 2018); and increases  
76 mortality (García-Hermoso *et al.*, 2018). There are no established therapeutics to slow  
77 musculoskeletal decline (Yoshimura *et al.*, 2017). Accordingly, the NIH identified a critical need  
78 (PAR-15-190) to “accelerate the pace of development of novel therapeutics... for preventing  
79 and treating key health issues affecting the elderly.”

80 The lack of effective therapeutics for musculoskeletal disorders is partially attributable to  
81 the insidious nature of musculoskeletal decline in humans, as well as the absence of animal  
82 models that recapitulate the multifactorial processes that drive musculoskeletal decline. The  
83 Hartley guinea pig is an outbred guinea pig that develops primary (also considered spontaneous  
84 or idiopathic) osteoarthritis (OA) starting at 4 months of age that closely resembles the onset  
85 and disease progression in humans (Jimenez *et al.*, 1997). By nine months of age, these guinea  
86 pigs have diminished mobility. At 18 months of age, the severity of OA renders the guinea pigs  
87 up to 50% less mobile (Santangelo *et al.*, 2014). Similar to humans with OA (Kemmler *et al.*,  
88 2015; Noehren *et al.*, 2018), skeletal muscle fiber size and density decrease and type I fibers  
89 increase by 15 months in these guinea pigs (Tonge *et al.*, 2013; Musci *et al.*, 2020), which in  
90 turn worsens the disease and contributes to disability in humans (Lee *et al.*, 2016). Thus, the  
91 Hartley guinea pig represents a potential model to study musculoskeletal deficiencies  
92 associated with osteoarthritis, an age-related chronic disease that affects over 30 million US

93 adults (United States Bone and Joint Initiative, 2020), in a compressed amount of time (i.e. 5 to  
94 15 months of age).

95 The musculoskeletal system is particularly susceptible to age-related declines in cellular  
96 function and increases in damage because it is slow to turnover relative to tissues such as liver  
97 (Drake *et al.*, 2013). Skeletal muscle is post mitotic and turnover of both bone tissue and  
98 cartilage is also slow (Vaananen, 1993; Hall, 2012; Relaix *et al.*, 2021). Thus, targeting the  
99 hallmarks of aging is likely particularly useful in counteracting age-related musculoskeletal  
100 dysfunction. For example, targeting mitochondrial dysfunction likely ameliorates not just  
101 impaired ATP production but also other, interconnected hallmarks of aging, such as impaired  
102 proteostasis (protein homeostasis) (Musci *et al.*, 2018). Impaired mitochondrial function is  
103 associated with, and precedes, impairments in proteostasis and decrements in skeletal muscle  
104 function (Gaffney *et al.*, 2018; Gonzalez-Freire *et al.*, 2018). Inversely, improvements in  
105 proteostatic mechanisms regulating mitochondrial proteome integrity would improve  
106 mitochondrial function (Hamilton & Miller, 2017), which would in turn alleviate the energetic  
107 constraints that impair adequate cellular function. This cyclical and interconnected relationship  
108 highlights the potential efficacy of targeting one hallmark of aging.

109 Nuclear factor erythroid 2-related factor 2 (Nrf2) is a transcription factor that regulates  
110 hundreds of genes involved in adaptation to stress, including those involved in redox  
111 homeostasis, mitochondrial energetics, and proteome maintenance (Gao *et al.*, 2020). Nrf2  
112 activation leads to the transcription of genes with the antioxidant response element in the  
113 promoter regions, including antioxidant genes such as SOD-1, NQO1, and HO-1 (Kobayashi &  
114 Yamamoto, 2006), has anti-inflammatory effects (Ahmed *et al.*, 2017), and has a role in  
115 regulating mitochondrial biogenesis (Piantadosi *et al.*, 2008). Transient Nrf2 activation through  
116 phytochemical supplementation (Donovan *et al.*, 2012; Reuland *et al.*, 2013; Kubo *et al.*, 2017;  
117 Hybertson *et al.*, 2019) is a potential therapeutic intervention that could mitigate age-related  
118 chronic diseases (Houghton *et al.*, 2016). Transiently activating Nrf2 targets several  
119 interconnected drivers of aging including macromolecular damage, disrupted redox homeostasis  
120 (Reuland *et al.*, 2013; Fang *et al.*, 2017), inflammation (Kobayashi *et al.*, 2016), and impaired  
121 proteostasis (Konopka *et al.*, 2017). In the NIH-NIA Interventions Testing Program (ITP),  
122 treatment with the phytochemical Nrf2 activator Protandim extended median lifespan of male  
123 mice (Strong *et al.*, 2016).

124 Given the positive effects of Nrf2 activator (Nrf2a) treatment, we sought to identify the  
125 effects of months-long Nrf2 activator treatment in the Hartley guinea pig. We hypothesized

126 Nrf2a treatment would improve skeletal muscle mitochondrial function and mechanisms of  
127 proteostasis and attenuate musculoskeletal declines in both male and female guinea pigs.

128 **Methods**

129 *Husbandry*

130 All procedures were approved by the Colorado State University Institutional Animal Care  
131 and Use Committee and were performed in accordance with the NIH Guide for the Care and  
132 Use of Laboratory Animals. Dunkin-Hartley guinea pigs were obtained from Charles River  
133 Laboratories (Wilmington, MA, USA) at 1- and 4- months of age (mo) for each treatment  
134 regimen such that there were 14 male and female guinea pigs in each age and treatment group  
135 (total n = 112) (Figure 1). As mentioned, Hartley guinea pigs begin developing knee OA at 4 mo  
136 and have severe OA and skeletal muscle and joint phenotypes consistent with aged human  
137 musculoskeletal systems by 15 mo (Jimenez *et al.*, 1997; Tonge *et al.*, 2013; Santangelo *et al.*,  
138 2014; Musci *et al.*, 2020). Accordingly, we chose these ages to determine if Nrf2a could prevent  
139 the onset (short term treatment from 2 to 5 mo) or mitigate the progression (long term treatment  
140 from 5 to 15 mo) of musculoskeletal dysfunction (Jimenez *et al.*, 1997; Santangelo *et al.*, 2014)  
141 and skeletal muscle decline (Musci *et al.*, 2020) (Figure 1). It is important to note that because  
142 knee OA was progressing as these animals age, we cannot discern the effect of age from  
143 disease progression or vice-versa. Thus, for any documented effect of age, we must also  
144 acknowledge that the effect could be attributed to disease progression.

145 Animals were maintained at Colorado State University's Laboratory Animal Resources  
146 housing facilities and were monitored daily by veterinary staff. All guinea pigs were singly-  
147 housed in solid bottom cages, maintained on a 12-12 hour light-dark cycle, and provided ad  
148 libitum access to food and water. Two control females, two Nrf2a females, one control male,  
149 and two Nrf2a males required humane euthanasia prior to final analysis due to underlying  
150 issues unrelated to treatment (final n = 105). Gross necropsy findings by veterinarians did not  
151 raise significant concern as the cause of death in these cases were consistent with what would  
152 be expected in conventionally raised guinea pigs.

153 *Measurement of PB125 in OraSweet and in Guinea Pig Plasma using High Performance Liquid  
154 Chromatography- Mass Spectrometry (HPLC/MS )*

155 PB125 (Pathways Bioscience, Aurora, CO) is a phytochemical compound comprised of  
156 rosemary, ashwagandha, and luteolin powders which contain the three active ingredients  
157 carnosol (CRN), withaferin A (WFA), and luteolin (LUT) at a mixed ratio of 15:5:2 by mass,  
158 respectively (Hybertson *et al.*, 2019). Prior to treatment initiation, plasma levels of each activate  
159 ingredient were measured 15, 30, 45, 60, 90, and 120 min post dosing at concentrations of 8,

160 24, and 48 mg/ml (Supplemental Figures 1A – 1C), which corresponds with a dosage of 250,  
161 750, and 1250 PPM. Compound stability in OraSweet was assessed both at room temperature  
162 and 4 °C. Reference standards of LUT and WFA were purchased from Sigma Aldrich (St. Louis,  
163 MO). CRN was purchased from Cayman Chemical (Ann Arbor, MI). All other reagents were  
164 purchased from Thermo Fisher Scientific (Waltham, MA). HPLC grade methanol was used for  
165 preparation of all solutions. Samples were analyzed at the Nathan Shock Core Analytical  
166 Pharmacology Core at the University of Texas Health Medical School.

167 The liquid chromatography tandem mass spectrometry (LC/MS/MS) system consisted of  
168 a Shimadzu SIL 20A HT autosampler, LC-20AD pumps (2), and an AB Sciex API 4000 tandem  
169 mass spectrometer with turbo ion spray. The LC analytical column was an ACE C8 (50 x 3.0  
170 mm, 3 micron) purchased from Mac-Mod Analytical (Chaddsford, PA). Mobile phase A  
171 contained 0.1% formic acid dissolved in water. Mobile phase B contained 0.1% formic acid  
172 dissolved in 100% HPLC grade acetonitrile. The LC Gradient was: 0 to 2 min, 25% B; 2 to 6  
173 min, linear gradient to 99% B; 6 to 10 min, 99% B; 10 to 10.01 min, 99% to 25% B min; 10.1 to  
174 12 min, 25% B. LUT and CRN were detected in negative mode using these transitions: 285 to  
175 132.9 m/z and 329 to 285 m/z, respectively. WFA was detected in positive mode at the  
176 transition of 471 to 281 m/z.

177 LUT, CRN, and WFA stock solutions were prepared in methanol at a concentration of 1  
178 mg/ml and stored in aliquots at -80 °C. Working stock solutions of each drug were prepared  
179 each day from the super stock solutions at a concentration of 100 µg/ml, 10 µg/ml, and 1 µg/ml  
180 which were used to spike the calibrators.

181 Dosages of PB125 in OraSweet were diluted 1000x in 70% ethanol. Calibrator samples  
182 were prepared daily by spiking blank OraSweet to achieve final concentrations of 0, 30.4, 152,  
183 760, and 2280 µg/ml. The calibrators were then diluted 1000x in 70% ethanol. The samples  
184 were transferred to injection vials and 10 µl was injected into the system. Each drug was  
185 quantified by comparing the peak area ratios for each dosage sample against a linear  
186 regression of calibrator peak area ratios. The concentration of each drug was reported as µg/ml.  
187 Because we prepared weekly allotments of PB125 in OraSweet, we verified the stability of  
188 PB125 suspended in OraSweet stored in 4°C for one week (Supplemental Figure 1D).

189 LUT, CRN, and WFA were also quantified in guinea pig plasma. The transitions used  
190 were the same as the OraSweet dilutions. Calibrator samples were prepared daily by spiking  
191 blank plasma to achieve final concentrations of 0, 5, 10, 25, 50, 100, 500, 1000, and 5000  
192 ng/ml. Calibrators were left to sit for 5 min after spiking. Briefly, 0.1 mL of calibrator and  
193 unknown plasma samples were mixed with 1.0 ml of chilled ethanol, vortexed vigorously, and

194 then centrifuged at 17,000 g for 5 min at 25 °C. The supernatants were transferred to 1.5 ml  
195 microcentrifuge tubes and dried to residue under a nitrogen stream. The residues were then  
196 redissolved in 60 µL of 50/50 mobile phase A/mobile phase B and were centrifuged 5 min at  
197 17,000 g. The samples were transferred to injection vials and 15 µL was injected into the  
198 LC/MS/MS. Each drug was quantified by comparing the peak area ratios for each unknown  
199 sample against a linear regression of calibrator peak area ratios. The concentration of LUT,  
200 CRN, and WFA were expressed as ng/mL plasma (Supplemental Figure 1A – C).

201 *Treatment, euthanasia, and tissue acquisition*

202 Based on the analysis conducted at the NSC Analytical Pharmacology Core  
203 (Supplemental Figure 1A – C), we selected a dosage of 8 mg/kg of bodyweight, which  
204 corresponds to 250 PPM, about 2.5x the dose of PB125 mice in the NIA ITP receive  
205 (<https://www.nia.nih.gov/research/dab/interventions-testing-program-itp/compounds-testing>).  
206 This dose was adequate to stimulate Nrf2 activation based on an increase in Nrf2 protein  
207 content in the gastrocnemius in a subset of both male and female guinea pigs (Supplemental  
208 Figure 1E). Nrf2 contains an antioxidant response element (ARE) promoter region, which  
209 activated Nrf2 proteins bind to upon activation and translocation into the nucleus. Because we  
210 were interested in long term effects of Nrf2 treatment (Miller *et al.*, 2016), we measured protein  
211 concentration instead of mRNA transcript concentration of a downstream Nrf2 target.  
212 Additionally, the last dose of the Nrf2 activator was 24 h prior to harvest, which precludes from  
213 measuring transcriptional responses to the PB125 treatment. After a one-month acclimation to  
214 housing conditions, male and female guinea pigs in each age group (2 or 5 months) were  
215 randomized to receive a daily oral dose of 8.0 mg/kg bodyweight of PB125 (Nrf2a) suspended in  
216 OraSweet (Perrigo, Dublin, Ireland) or an equivalent volume of OraSweet only (CON). Following  
217 established protocol, guinea pigs were given a subcutaneous injection of 0.9% saline enriched  
218 with 99% deuterium ( $^2\text{H}_2\text{O}$ ) equivalent to 3% of their body weight 30 days prior to euthanasia  
219 (Minci *et al.*, 2020). Drinking water was enriched to 8%  $^2\text{H}_2\text{O}$  for the purpose of maintaining  
220  $^2\text{H}_2\text{O}$  enrichment of the body water pool during the 30-day labelling period. At the time of  
221 harvest, the guinea pigs were 5 mo (after 3 months of treatment) or 15 mo (after 10 months of  
222 treatment of age). In accordance with the standards of the American Veterinary Medical  
223 Association, animals were anesthetized with a mixture of isoflurane and oxygen; thoracic  
224 cavities were opened and blood was collected via direct cardiac puncture. Whole blood was  
225 centrifuged (1200 g, 4 °C, 15 min) to separate plasma, which was frozen at -80 °C until further  
226 analysis. After blood collection, the anesthetized animals were transferred a chamber filled with  
227 carbon dioxide for euthanasia.

228       Upon euthanasia, the right leg of the guinea pig was promptly removed for the excision  
229       of the soleus muscle. A portion of the right soleus muscle (~40 mg) was harvested and placed  
230       in BIOPS preservation buffer (2.77 mM CaK2-EGTA, 7.23 mM K2-EGTA, 20 mM imidazole, 20  
231       mM taurine, 50 mM K-MES, 0.5 mM dithiothreitol, 6.56 mM MgCl<sub>2</sub>, 5.77 mM ATP, and 15 mM  
232       phosphocreatine, adjusted to pH 7.1) containing 12.5  $\mu$ M blebbistatin to inhibit muscle  
233       contraction (Pesta & Gnaiger, 2011). The rest (~70 mg) of the soleus was frozen in liquid  
234       nitrogen and used for other analyses. After excision of the soleus, at least 70 mg of the right  
235       gastrocnemius was collected and frozen immediately in liquid nitrogen. Both soleus and  
236       gastrocnemius muscles were trimmed of tendons and connective tissue and weighed. Bone  
237       marrow was also harvested in saline from the humeri.

238       *Mitochondrial respirometry*

239       After the soleus was placed in BIOPS, the muscle fibers were prepared for high  
240       resolution respirometry as follows. Mechanical permeabilization occurred on ice using forceps to  
241       separate the fibers. After mechanical permeabilization, fibers underwent chemical  
242       permeabilization for 30 min in BIOPS with 12.5  $\mu$ M blebbistatin and 50  $\mu$ g/mL saponin, followed  
243       by a 15 min rinse in BIOPS. Approximately 2.0 mg (wet weight) of muscle fibers were placed in  
244       mitochondrial respiration medium (MiR05, 0.5 mM EGTA, 3 mM MgCl<sub>2</sub>6H<sub>2</sub>O, 20 mM Taurine, 15  
245       mM Na<sub>2</sub>Phosphocreatine, 20 mM Imidazole, 0.5 mM Dithiothreitol, and 50 mM K<sup>+</sup> -MES at pH  
246       7.1) in an Oxygraph-2k (O2K) (Oroboros, Innsbruck, Austria) for high resolution respirometry.  
247       To control for oxygen flux at higher concentrations of oxygen, each morning of respirometry  
248       analysis, we conducted high oxygen concentration calibrations at 450, 350, 250, and 167 (i.e.,  
249       concentration of room air) nmol/ml O<sub>2</sub> (Pesta & Gnaiger, 2011). During the experiments, oxygen  
250       concentrations were maintained between 225 – 450 nmol/ml O<sub>2</sub>. High resolution respirometry  
251       measurements were performed in duplicate using two different protocols. Please refer to  
252       Supplemental Table 1 for a detailed explanation of the protocols.

253       The first protocol (SUIT 1) was an ADP titration protocol to determine ADP sensitivity  
254       (K<sub>m</sub>) and maximal oxidative capacity (V<sub>max</sub>) under Complex I supported respiration. We  
255       measured Complex I supported leak respiration (State 2<sub>[PGM]</sub>) with the addition of 10 mM  
256       glutamate, 0.5 mM malate, and 5 mM pyruvate. Upon acquisition of State 2<sub>[PGM]</sub>, we titrated  
257       progressively greater concentrations of ADP from 0.1 mM, 0.175 mM, 0.25 mM, 1 mM, 2 mM, 4  
258       mM, 8 mM, 12 mM, 20 mM, to 24 mM (State 3<sub>[PGM]</sub>), awaiting steady-state oxygen flux prior to  
259       adding the subsequent titration to determine Complex I linked ADP V<sub>max</sub> and apparent K<sub>m</sub> (i.e.  
260       ADP sensitivity). After the ADP titration was completed, we added 5 mM cytochrome C to test  
261       mitochondrial membrane integrity. After cytochrome C addition, we added 10 mM succinate to

262 acquire maximal Complex I and II supported coupled respiration (State 3<sub>[PGM + S]</sub>). We then  
263 added 0.5  $\mu$ M FCCP sequentially until there was no increase in respiration to determine the  
264 capacity of the electron transport system to consume oxygen, or maximal uncoupled respiration  
265 (ETS<sub>[CI-ClV]</sub>). Finally, we added 5  $\mu$ M rotenone to measure maximal uncoupled respiration with  
266 the inhibition of Complex I (ETS<sub>[CII-ClV]</sub>), followed by 2.5  $\mu$ M Antimycin A to measure residual  
267 oxygen consumption (ROX).

268 The second protocol (SUIT 2) measured oxygen consumption while simultaneously  
269 measuring ROS production by using the fluorometer attachment of the O2K (Robinson *et al.*,  
270 2019) and addition of 10  $\mu$ M Amplex Red, 1 U/ml horseradish peroxidase, and 5 U/ml  
271 superoxide dismutase. We then measured fatty acid supported leak respiration by adding 10  
272 mM glutamate, 0.5 mM malate, 5 mM pyruvate, and 0.2 mM octanoylcarnitine (State 2<sub>[PGM + Oct]</sub>)  
273 and 10 mM succinate (State 2<sub>[PGM + Oct + S]</sub>). After stimulating maximal leak respiration, we added  
274 submaximal boluses of ADP (0.5 mM: (State 3<sub>[Sub + 0.5D]</sub>) and 1 mM: State 3<sub>[Sub + 1.0D]</sub>), followed by  
275 a saturating bolus of ADP (6.0 mM: State 3<sub>[Sub + 6.0D]</sub>). We added 5 mM cytochrome C to test  
276 mitochondrial membrane integrity. We set a cytochrome C control factor threshold of 0.25. We  
277 set this threshold based on the presence of a negative linear relationship between the  
278 cytochrome C control factor and State 3 respiration in the SUIT 2 protocol. Upon eliminating  
279 respirometry trials that had a cytochrome C control factor of greater than 0.25, the negative  
280 linear relationship no longer existed and all samples included in analysis were not biased by  
281 over-permeabilization, which is what the cytochrome C control factor approximates (Pesta &  
282 Gnaiger, 2011) (Supplemental Figure 4 A - C). We then added 5  $\mu$ M rotenone to determine  
283 maximal coupled respiration in the absence of Complex I (State 3<sub>[Sub + D - CI]</sub>) followed by  
284 sequential titrations of 0.5  $\mu$ M FCCP until respiration no longer increased to determine maximal  
285 fatty acid supported uncoupled respiration (ETS<sub>[Sub + D - CI]</sub>). and added 2.5  $\mu$ M antimycin A to  
286 measure ROX. The respiratory control ratio (RCR: State 3/State 2), which is an index of  
287 mitochondrial efficiency was also evaluated.

288 *Protein isolation and fractionation*

289 The gastrocnemius and soleus muscles were homogenized and fractionated following  
290 established laboratory protocols (Drake *et al.*, 2013; Miller *et al.*, 2013; Groennebaek *et al.*,  
291 2018; Sieljacks *et al.*, 2019; Musci *et al.*, 2020). Briefly, tissues (20 – 50 mg) were homogenized  
292 at 1:10 in isolation buffer (100 mM KCl, 40 mM Tris HCl, 10 mM Tris Base, 5 mM MgCl<sub>2</sub>, 1 mM  
293 EDTA, 1 mM ATP, pH – 7.5) with phosphatase and protease inhibitors (HALT Thermo Scientific,  
294 Rockford, IL, USA) using a tissue homogenizer (Bullet Blender, Next Advance Inc., Averill Park,  
295 NY, USA) with zirconium beads (Next Advance Inc., Averill Park, NY, USA). After

296 homogenization, subcellular fractions were isolated via differential centrifugation as previously  
297 described (MUSCI *et al.*, 2020). Once fractionated pellets were isolated and purified, 250  $\mu$ L 1 M  
298 NaOH was added and pellets were incubated for 15 min at 50 °C and 900 RPM.

299 *DNA extraction*

300 Approximately 100 ng/ $\mu$ L of total DNA was extracted from 20 mg tissue (QiAMP DNA  
301 mini kit Qiagen, Valencia, CA, USA). DNA from bone marrow was extracted from the bone  
302 marrow suspension and centrifuged for 10 min at 2000 g, yielding approximately 100 ng/ $\mu$ L.

303 *Sample preparation and analysis via GC/MS: Proteins*

304 Protein subfractions were hydrolyzed in 6 M HCl for 24 hours at 120 °C after which the  
305 hydrolysates were ion-exchanged, dried *in vacuo*, and then resuspended in 1 mL of molecular  
306 biology grade H<sub>2</sub>O. Half of the suspension was derivatized with 500  $\mu$ L acetonitrile, 50  $\mu$ L 1 M  
307 K<sub>2</sub>HPO<sub>4</sub>, and 20  $\mu$ L of pentafluorobenzyl bromide and incubated at 100 °C for 60 min.  
308 Derivatives were extracted into ethyl acetate and the organic layer was transferred into vials  
309 which were then dried under nitrogen. Samples were reconstituted in ethyl acetate (200  $\mu$ L –  
310 700  $\mu$ L).

311 The derivative of alanine was analyzed on an Agilent 7890A GC coupled to an Agilent  
312 5977A MS as previously described (ROBINSON *et al.*, 2011; DRAKE *et al.*, 2013; MILLER *et al.*, 2013;  
313 GROENNEBAEK *et al.*, 2018; MILLER *et al.*, 2019; SIELJACKS *et al.*, 2019; MUSCI *et al.*, 2020). The  
314 newly synthesized fraction (f) of proteins was calculated from the true precursor enrichment (p)  
315 based upon plasma analyzed for <sup>2</sup>H<sub>2</sub>O enrichment and adjusted using mass isotopomer  
316 distribution analysis (BUSCH *et al.*, 2005). Protein synthesis of each subfraction was calculated  
317 as the fraction of deuterium-labeled over unlabeled alanine proteins over the entire labeling  
318 period (30 days) and expressed as the fractional synthesis rate (FSR). Thus, we divided fraction  
319 new by our labeling period (30 days) and multiplied by 100 to express FSR as %/day. Our  
320 isotope approach and analysis followed the established procedures detailed in this Core of  
321 Reproducibility in Physiology publication (MILLER *et al.*, 2020).

322 *Sample preparation and analysis via Gas Chromatography/Mass Spectroscopy (GC/MS): Body  
323 water*

324 80  $\mu$ L of plasma was placed into the inner well of an o-ring cap that was screwed to tube  
325 and inverted on a heating block overnight at 100 °C. After incubation, 2  $\mu$ L of 10 M NaOH and  
326 20  $\mu$ L of acetone were added to the samples and <sup>2</sup>H<sub>2</sub>O standards (0 – 20%) and capped  
327 immediately, vortexed, and incubated at room temperature overnight. Samples were extracted  
328 with 200  $\mu$ L hexane and the organic layer was transferred through pipette tips filled with  
329 anhydrous Na<sub>2</sub>SO<sub>4</sub> into GC vials and analyzed via EI mode using a DB-17MS column.

330 *Sample preparation and analysis via GC/MS: DNA*

331        Incorporation of  $^2\text{H}$  into purine deoxyribose (dR) of DNA was measured follow  
332 procedures already described (Busch *et al.*, 2007; Miller *et al.*, 2012; Drake *et al.*, 2013; Drake  
333 *et al.*, 2014). DNA that was isolated from tissue and bone marrow were hydrolyzed with  
334 nuclease S1 and potato acid phosphatase at 37 °C shaking at 150 RPM overnight. These  
335 hydrolysates were derivatized with pentafluorobenzyl hydroxylamine and acetic acid and  
336 incubated at 100 °C for 30 min. After incubation, samples were acetylated with acetic anhydride  
337 and 1-methylimidazole. Dichloromethane was added, mixed and then extracted, dried *in vacuo*,  
338 and resuspended in ethyl acetate, and analyzed by GC/MS as previously described (Busch *et*  
339 *al.*, 2007; Miller *et al.*, 2012; Drake *et al.*, 2014; Drake *et al.*, 2015). The fraction new was  
340 calculated by dividing deuterated dR of the muscle tissue by the bone marrow of the same  
341 animal, which represents a fully turned-over cell population, and thus indicative of precursor  
342 enrichment (Miller *et al.*, 2012; Miller *et al.*, 2014; Drake *et al.*, 2015).

343 *Assessing protein synthesis related to mechanisms of proteostasis*

344        To evaluate protein synthesis related to protein maintenance versus new cell  
345 proliferation (new DNA), we calculated the ratio of protein synthesis to DNA synthesis (Drake *et*  
346 *al.*, 2014; Miller *et al.*, 2014; Drake *et al.*, 2015; Hamilton & Miller, 2017). Increases in PRO:DNA  
347 is indicative of a greater proportion of protein synthesis related to protein turnover to maintain  
348 the proteome, with less dedicated to proliferation.

349 *Protein content*

350        Western blotting was used to measure relative content of Nrf2 and OXPHOS proteins in  
351 a subset of tissues. 50-70 mg portions of gastrocnemius and 30 mg portions of soleus (n=9 per  
352 treatment group) were powdered under liquid nitrogen and homogenized in a Bullet Blender with  
353 zirconium beads and 1.0 mL of radioimmunoprecipitation assay (RIPA) buffer (150 mM NaCl,  
354 0.1 mM EDTA, 50 mM Tris, 0.1% sodium deoxycholate, 0.1% SDS, 1% Triton X-100, pH = 7.50)  
355 with HALT protease inhibitors. Samples were reduced (50  $\mu\text{L}$  of B-mercaptoethanol) and heated  
356 at 50 °C for 10 min. Approximately 10  $\mu\text{g}$  of protein was loaded into a 4% - 20% Criterion pre-  
357 cast gel (Bio-Rad, Hercules, CA, USA) and resolved at 120 V for 120 min. The proteins were  
358 then transferred to a PVDF membrane at 100 V for 75 min in transfer buffer (20% w/v methanol,  
359 0.02% w/v SDS, 25 mM Tris Base, 192 mM glycine, pH 8.3). Protein transfer to membrane was  
360 confirmed with ponceau stain. Membranes were then blocked and incubated with primary  
361 antibodies against Nrf2 (Santa Cruz 13032) and total OXPHOS proteins (Abcam 110413)  
362 diluted to 1:500 on a shaker overnight in 4 °C. Membranes were rinsed and then incubated with  
363 appropriate secondary antibodies (Santa Cruz 2004 and 2005, respectively) diluted to 1:10,000

364 for 45 min at room temperature. Protein carbonyls were measured by following the protocol in  
365 the commercially available OxiSelect Protein Carbonyl Immunoblot Kit (Cell Biolabs STA-308)  
366 as previously performed (Konopka *et al.*, 2015; Konopka *et al.*, 2017). After the membranes  
367 were rinsed, SuperSignal West Dura Extended Duration Substrate (Thermo Fisher 34075) was  
368 applied and the membranes were subsequently imaged using a FluorChem E  
369 Chemiluminescence Imager (Protein Simple, San Diego, CA, USA). Analysis of densitometry  
370 was completed using AlphaView SA Software. Units are expressed as density of primary  
371 antibody relative to density of ponceau staining.

372 *Mobility*

373 Animals were acclimated over a 2-week period, before the onset of the study, to an open  
374 circular field behavior monitoring system (ANY-maze<sup>TM</sup>, Wood Dale, IL) to assess voluntary  
375 physical mobility. Animals' activities were recorded, and data were collected for 10 consecutive  
376 minutes on a monthly basis throughout the study. Videos were analyzed for the following  
377 parameters: total distance traveled (m), average speed (m/s), time mobile (s), % time mobile,  
378 time in hut (s), % time in hut, and average moving speed (m/s). Because musculoskeletal  
379 degradation causes immobility in Hartley guinea pigs, Kaplan Meier curves combined with log  
380 rank and Gehan-Breslow-Wilcoxon tests were utilized to assess the probability of sustained  
381 voluntary mobility throughout the 10-month study period of the "long term" study. The "event"  
382 was task noncompliance and defined as number of weeks into the study until an animal did not  
383 move (i.e., zero distanced traveled when exposed to the open circular field). Remaining  
384 individuals that maintained mobility throughout the entire 40-week study duration were censored  
385 at the 40-week study endpoint.

386 *Statistics*

387 For mitochondrial respirometry, in line with best practices, technical replicates were  
388 averaged. The average variability between these technical replicates in this study was 18%,  
389 which is standard according to the literature (Jacques *et al.*, 2020). Apparent Km and Vmax  
390 values were determined using Michaelis-Menten kinetics in Prism 9.0 (La Jolla, California,  
391 USA). For evaluating growth rates, a non-linear Gompertz growth line was fit to the change in  
392 body mass over time (i.e. the rate of growth). The rate of growth, k, was compared between  
393 treatment and control within in each sex. For respirometry, isotopic measures, and Western  
394 blots, three-way ANOVAs were used to measure the main effects of sex, disease/age, and  
395 Nrf2a treatment. Post-hoc analyses were performed using Bonferroni's post-hoc test.

396 To determine the effect of Nrf2a on disease/age-related changes in mitochondrial  
397 respiration and protein synthesis when a significant effect of disease/age was detected, we

398 conducted a subset analysis using a one-way ANOVA with a Dunnett's post-hoc test comparing  
399 15 mo treated and untreated guinea pigs to 5 mo untreated guinea pigs.

400 To assess treatment and sex effects in PRO:DNA of 15 mo guinea pigs, we used a Two-  
401 Way ANOVA. We excluded 5 mo guinea pigs from this analysis because of the significantly  
402 greater DNA fraction new in 5 mo guinea pigs compared to 15 mo guinea pigs, which makes the  
403 age-related comparison of PRO:DNA less relevant. Due to sample loss during processing of  
404 bone marrow, there is a reduced sample size for DNA fraction new outcomes, which also  
405 affected PRO:DNA.

406 For Western blots, a subset (n=9) of guinea pigs were randomly selected for analysis.  
407 Because this study was a secondary project within a larger study with a different primary  
408 outcome, we did not design this study to be powered to detect differences in mitochondrial  
409 respiration and protein synthesis at a p-value <0.05. While we set statistical significance *a priori*  
410 at p<0.05, we also report differences with p<0.10 to highlight potential directions for future  
411 studies. Data are presented as mean +/- SD. All statistics were performed in Prism 9.0 (La Jolla,  
412 California, USA).

### 413 **Results**

414 Growth rate (k-curves) of the group treated with PB125 (Nrf2a) did not significantly differ  
415 from the control group (CON) as measured by changes of body weight throughout treatment  
416 (p>0.70 for both sexes) and body mass at harvest (p>0.70) (Supplemental Figures 2A - C).  
417 Skeletal muscle DNA synthesis, which is reflective of proliferation of various cell types within the  
418 skeletal muscle niche, also was not different between Nrf2a and CON (Supplemental Figure 2D  
419 - E). Moreover, there were no differences in absolute or relative skeletal muscle mass between  
420 Nrf2a and CON (Supplemental Figure 3).

421 *Disease/age-related declines in mitochondrial respiration are not sex-specific in Hartley guinea  
422 pigs*

423 Because mitochondrial respiratory capacity has never been measured in permeabilized  
424 skeletal muscle fibers from Hartley guinea pigs, we first evaluated disease/age- and sex-  
425 differences in mitochondrial respiration. As a reference, refer to Supplemental Table 1 for a  
426 glossary and detailed titration data for respiratory state mentioned below. Eleven of 210 trials  
427 were excluded due to over-permeabilization (cytochrome C control factor > 0.25; Supplemental  
428 Figures 4A - B). Maximal coupled (State 3<sub>[CI-CIV]</sub>) (Figure 2A) and uncoupled (Electron Transport  
429 System (ETS) <sub>[CI-CIV]</sub>) (Figure 2B) respiration were significantly greater in males (p=0.006;  
430 p=0.002, respectively). Uncoupled Complex II-IV (ETS<sub>[CII-CIV]</sub>) supported respiration was greater  
431 in males than females (Figure 2C) (p=0.002). However, there was no difference in mitochondrial

432 efficiency (RCR) between sexes (Figure 2D). Males have greater fatty acid supported coupled  
433 respiration at sub-saturating (1 mM ADP) and saturating (6 mM ADP) concentrations of ADP  
434 (p=0.024 and p=0.018, respectively) (Figures 3B - C).

435 Disease/age had a negative effect on several aspects of mitochondrial function in both  
436 male and female guinea pigs. 15 mo male and female guinea pigs had lower coupled (State  
437 3<sub>[PGM+S]</sub>) (Figure 2A) and uncoupled (ETS<sub>[CI-CIV]</sub>) (Figure 2B) respiration (p=0.001, p=0.004,  
438 respectively). There was also a disease/age-related decline (p<0.0001) in uncoupled respiration  
439 without Complex I support (ETS<sub>[CII-CIV]</sub>) (Figure 2C). Disease/age had no effect on fatty acid  
440 oxidation supported respiration at sub-saturating levels ADP (Figures 3A – B), though 15 mo  
441 guinea pigs had lower fatty acid oxidation supported respiration at saturating levels of ADP  
442 (Figure 3C; p=0.056). Mitochondrial efficiency (RCR) also decreased as a result of disease/age  
443 (p=0.012) (Figure 2D).

444 *Nrf2a improves mitochondrial respiration in both male and females*

445 Nrf2a improved several components of mitochondrial respiration in both 5 mo and 15 mo  
446 guinea pigs, and in both males and females. Nrf2a did not significantly enhance coupled  
447 respiration (State 3[PGM+S]) in male and female guinea pigs (p=0.098) (Figure 2A), but did  
448 significantly increase electron transport system (ETS) capacity (ETS<sub>[CI-CIV]</sub>) (Figure 2B; p=0.037).  
449 However, Nrf2a did not influence uncoupled respiration with Complex I inhibited (ETS[CII-CIV])  
450 (Figure 2C).

451 Nrf2a did not significantly improve fatty acid supported respiration at sub-saturating (1  
452 mM ADP) and saturating (6 mM ADP) concentrations of ADP (Figures 3B - C; p=0.061,  
453 p=0.074, respectively). There was no main effect of Nrf2a on RCR (Figure 2D), a metric of  
454 mitochondrial efficiency, or on ROS emission (Supplemental Figure 5).

455 *Nrf2a has sex specific effects on mitochondrial ADP kinetics*

456 No O2K data from the ADP titration protocol were excluded based on cytochrome C  
457 control factors as all values were below 0.25 (Supplemental Figure 4C). We determined ADP  
458 kinetics by titrating progressively higher concentrations of ADP with saturating amounts of  
459 pyruvate, glutamate, and malate (titration curves found in Supplemental Figure 6E – H). ADP  
460 Vmax was greater in both 15 mo male and female guinea pigs compared to 5 mo counterparts  
461 (p=0.049) (Figure 4A). In females, ADP Vmax was lower compared to males (p=0.001) (Figure  
462 4A). Guinea pigs that received treatment with the Nrf2 activator (Nrf2a) had a greater Complex I  
463 supported ADP Vmax. Post-hoc comparisons indicate that Nrf2a improved ADP Vmax in 5 mo  
464 female guinea pigs (p=0.045).

465           Despite ADP Vmax being greater in 15 mo guinea pigs, there was no effect of  
466 disease/age on the apparent Km of ADP (Figure 4B). There were also no differences in Km  
467 between sexes. However, Nrf2a did significantly increase the apparent Km ( $p=0.007$ ) indicating  
468 lower ADP sensitivity, though this is likely a consequence of increased ADP Vmax in the  
469 absence of changes in respiration rates in sub-saturating amounts of ADP (Supplemental Figure  
470 6). There was non-significant interaction between sex and Nrf2a treatment ( $p=0.092$ ), indicating  
471 that the Nrf2a-mediated decrease in Km may have occurred only in males.

472 *Nrf2a attenuates age-related declines in mitochondrial respiration*

473           For any main effects of disease/age on mitochondrial respiration, we evaluated if Nrf2a  
474 attenuated the age-related changes. That is, where we identified significant differences between  
475 5 mo CON and 15 mo CON guinea pigs, but no differences between 5 mo CON and 15 mo  
476 Nrf2a animals, we reported those findings as an attenuating effect of Nrf2a treatment on age-  
477 related changes in mitochondrial function. While there was a main positive effect of age on ADP  
478 Vmax in the three-way ANOVA (Figure 4A), there was no difference in ADP Vmax between 5  
479 mo and 15 mo CON guinea pigs ( $p=0.109$ ) in the subsequent one-way ANOVA analysis (Figure  
480 5A). Treated 15 mo guinea pigs, however, had a significantly higher ADP Vmax compared to 5  
481 mo animals ( $p=0.007$ ) (Figure 4A). Interestingly, this effect was only observed in males  
482 ( $p=0.021$ ) (Figure 5B). While ADP Vmax was greater in 15 mo guinea pigs, 15 mo guinea pigs  
483 had a significantly ( $p=0.024$ ) lower maximal coupled respiration (State 3<sub>[C1-CIV]</sub>) compared to 5  
484 mo counterparts (Figure 5C). Nrf2a, however, prevented that disease/age-related decline  
485 (Figure 5C). Maximal uncoupled respiration (ETS<sub>[C1-CIV]</sub>) was also lower between 5 mo and 15  
486 mo CON (Figure 5E), but Nrf2a prevented the decline. Further interrogation revealed that 15 mo  
487 females had lower ETS<sub>[C1-CIV]</sub> compared to their 5 mo counterparts, which Nrf2a attenuated  
488 (Figure 5F). Interestingly, when Complex I was inhibited, Nrf2a had no effect on uncoupled  
489 respiration (ETS<sub>[CII-CIV]</sub>) and had no effect on the disease/age-related decline in CII-CIV capacity  
490 in either 15 mo males ( $p=0.035$ ) or females ( $p=0.003$ ) (Figures 5G - H). While the RCR of 15 mo  
491 CON guinea pigs were lower compared to 5 mo guinea pigs, RCR was not different between 15  
492 mo Nrf2a treated guinea pigs and 5 mo CON (Figure 5I). However, this occurred only in males  
493 where there was a significant difference ( $p=0.036$ ) between 5 mo and 15 mo CON animals  
494 (Figure 5J) but no difference ( $p=0.151$ ) between 15 mo males treated with Nrf2a compared to 5  
495 mo CON (Figure 5J). There was no difference in RCR between 5 mo and 15 mo females  
496 (Figure 5J). Altogether, these data support that Nrf2a can attenuate age related declines in  
497 mitochondrial respiration. Interestingly, Nrf2a had no effect on mitochondrial content as  
498 assessed by Western blot (Supplemental Figure 7), suggesting that the improvements in

499 mitochondrial function are independent of mitochondrial content in skeletal muscle and may  
500 reflect improved mitochondrial quality.

501 *Age- sex- and treatment- related effects on skeletal muscle protein synthesis*

502 To determine whether or not Nrf2a-mediated improvement in mitochondrial respiration  
503 was linked to improvements in components of proteostasis, we used  $^{2}\text{H}_2\text{O}$  to measure  
504 cumulative protein and DNA synthesis rates over 30 days. There were no differences in  
505 fractional synthesis rate (FSR) in either the gastrocnemius or soleus between male and female  
506 guinea pigs (Figure 6). There was a disease/age-related decline in the rates of protein synthesis  
507 in all subfractions in the soleus and gastrocnemius of both male and female guinea pigs ( $p<0.01$   
508 for all subfractions) (Figure 6). Nrf2a did not have a main effect on FSR in any of the  
509 subfractions of either muscle from 5 mo or 15 mo, male or female guinea pigs (Figure 6).  
510 However, there was a non-significant interaction between age and Nrf2a ( $p=0.086$ ) in the  
511 myofibrillar subfraction of the soleus of both male and female guinea pigs, suggesting that Nrf2a  
512 may have had a positive effect on myofibrillar FSR at 15 mo (Figure 6A).

513 *Nrf2a mitigates age-related declines protein synthesis*

514 Because there was a disease/age-related decline in protein synthesis rates in all  
515 subfractions of both the soleus and gastrocnemius, we sought to determine if Nrf2a prevented  
516 any of those declines. Nrf2a attenuated the disease/age-related decline in myofibrillar FSR of  
517 the soleus in both males and females (Figures 7A - B). Additionally, Nrf2a attenuated the  
518 decline in mitochondrial FSR in the soleus (Figure 7C), but these significant differences were no  
519 longer detectable when evaluated in males and females separately (Figure 7D). In the soleus,  
520 Nrf2a also mitigated the decline in cytosolic FSR in males only (Figure 7F), but had no effect on  
521 the decline in collagen FSR in either sex (Figures 7G - H). In contrast, Nrf2a had no attenuating  
522 effect on the disease/age-related decline in protein synthesis in any subfraction of the  
523 gastrocnemius (Figure 8).

524 *Nrf2a does not affect protein synthesis related to proteostasis*

525 Because protein synthesis is an essential process for both growth and proteostasis, it  
526 was necessary to discern the relative amount of protein synthesis allocated towards protein  
527 turnover (i.e. proteostasis). To do this, protein synthesis rates were evaluated relative to the  
528 rates of cell proliferation. An increased protein synthesis rate to DNA synthesis rate ratio  
529 (PRO:DNA) suggests a greater allocation of newly synthesized proteins associated with  
530 maintaining the cellular proteome, with less dedicated to new cell proliferation. In 5 mo guinea  
531 pigs, there was no effect of Nrf2a on the PRO:DNA in the gastrocnemius or soleus  
532 (Supplemental Figure 8). Similarly, there was no difference in PRO:DNA in 15 mo guinea pigs

533 (Figure 9). Given the constrained sample size due to loss of sample, further investigation is  
534 warranted. Given the lack of effect of Nrf2a on PRO:DNA, which is reflective of the proportion of  
535 proteins synthesized allocated to proteome maintenance, it is unsurprising that there were no  
536 differences in protein carbonyl content, a marker of protein damage, in the soleus or  
537 gastrocnemius (Supplemental Figure 9).

#### 538 *The effect of Nrf2a on mobility*

539 To determine whether or not improvements in skeletal muscle mitochondrial function and  
540 proteostasis translated to improvements in mobility, we assessed voluntary activity in a dark,  
541 enclosed area using overhead monitoring. Kaplan-Meier curves depicting the probability of  
542 sustained voluntary mobility throughout the 40-week study period. There was no statistically  
543 significant effect of Nrf2a on maintained mobility in either male or female guinea pigs. CON  
544 guinea pigs lost mobility more rapidly than Nrf2a guinea pigs (Figures 10A – B; grouped sex  
545 hazard ratio=0.713, 95% CI=0.3501 to 1.453; median ratio=1.5, CI=0.756 to 2.976; p=0.231).  
546 Further, Nrf2a males tend to have a relative increase in mobility compared to controls until  
547 about 32 weeks into the study. However, 50% of Nrf2a males lost mobility by 36 weeks, while  
548 50% of CON males maintained mobility the entire 40-week study duration (remaining animals  
549 were censored at this time) (Figure 10A). For the majority of the study, Nrf2a females  
550 maintained their mobility compared to CON females. Approximately 50% of control females loss  
551 mobility around 16 weeks, while Nrf2a treated females sustained voluntary mobility until about  
552 28 weeks (Figure 10B).

#### 553 **Discussion**

554 In this study, we tested the effects of a novel phytochemical Nrf2 activator, PB125 on  
555 two hallmarks of aging implicated in musculoskeletal decline in humans: mitochondrial  
556 dysfunction and loss of proteostasis in locomotor muscle. We observed that Nrf2 activator  
557 treatment (Nrf2a) ameliorated declines in skeletal muscle mitochondrial function and protein  
558 synthesis in both male and female Hartley guinea pigs as these guinea pigs age and develop  
559 knee OA. The improvements and maintenance of mitochondrial respiration and proteostatic  
560 mechanisms may also be associated with prolonged maintenance of voluntary activity in  
561 females. Collectively, this study demonstrates the potential utility of Nrf2 activators in targeting  
562 musculoskeletal decline.

#### 563 *Sex- and age/disease-related differences in mitochondrial respiration*

564 This is the first study to measure skeletal muscle mitochondrial function in either male or  
565 female Hartley guinea pigs using high resolution respirometry. Accordingly, we first sought to  
566 characterize differences between male and female guinea pigs at 5 and 15 months of age to

567 determine sex differences and age- and disease-related (i.e. worsening knee osteoarthritis)  
568 changes in skeletal muscle mitochondrial respiration. We found a clear sex difference in  
569 coupled and uncoupled respiration (females and lower rates of oxygen consumption than  
570 males), accompanied by decreased fatty acid supported respiration and ADP kinetics.  
571 Interestingly, these differences do not seem to be a consequence of differences in mitochondrial  
572 density and may instead reflect intrinsic differences in mitochondrial function. One study in both  
573 young and old men and women determined that there was no difference in phosphocreatine  
574 recovery post-exercise, a metric of mitochondrial capacity (Kent-Braun & Ng, 2000). However,  
575 measuring ATP production using bioluminescence revealed that mitochondria of men have  
576 greater capacity to produce ATP than that of women (Karakelides *et al.*, 2010). Employing high  
577 resolution respirometry has revealed equivocal results; thus, it remains unclear whether or not  
578 females have greater oxidative capacity than males (Cardinale *et al.*, 2018; Miotto *et al.*, 2018).  
579 Regardless, it is essential to continue interrogating potential sex differences in mitochondrial  
580 function and changes that occur with both age and disease in both sexes.

581 Mitochondrial function declines with age and contributes to the aging process in humans  
582 (Short *et al.*, 2005; Gonzalez-Freire *et al.*, 2015; Distefano *et al.*, 2017; Gonzalez-Freire *et al.*,  
583 2018). We demonstrated that both male and female Hartley guinea pigs similarly experience a  
584 decline in mitochondrial respiration as humans do. However, given the relatively early age of  
585 these guinea pigs (15 months; ~10% of recorded maximal lifespan (Gorbunova *et al.*, 2008),  
586 and ~25% of average companion guinea pig lifespan (Quesenberry *et al.*, 2021)), is difficult to  
587 ascertain if these changes are a consequence of either age, a consequence of the underlying  
588 factors that drive osteoarthritis and musculoskeletal dysfunction, or a combination of both. Other  
589 laboratory and companion animal guinea pigs do not exhibit such phenotypes as early in their  
590 lifespans (Santangelo *et al.*, 2011; Musci *et al.*, 2020). Notably, osteoarthritis is associated with  
591 impaired mitochondrial function and redox metabolism in degenerating joints (Loeser, 2010;  
592 Collins *et al.*, 2016; Farnaghi *et al.*, 2017; Collins *et al.*, 2018). In the current study, both coupled  
593 and uncoupled respiration, as well as mitochondrial efficiency, declined with age/disease  
594 progression in both male and female guinea pig skeletal muscle (Figures 2A – D). There was  
595 also a decline in fatty acid supported oxidation (Figure 3C). In contrast, ADP Vmax  
596 unexpectedly increased with age in both male and female guinea pigs. Given the non-uniform  
597 changes in mitochondrial complex protein content (Supplemental Figure 7F – J), it is unclear if  
598 differences in mitochondrial density explain the age/disease-related declines in respiration.  
599 However, these data clearly demonstrate that impaired mitochondrial respiration is a  
600 characteristic of this pre-clinical model of musculoskeletal decline.

601 *Nrf2 activator treatment ameliorates age-related declines in mitochondrial respiration*  
602 Nrf2a treated guinea pigs had augmented mitochondrial function in 5 mo females and 15  
603 mo males as characterized greater ADP Vmax and electron transport system capacity  $ET_{[CI-CIV]}$ . Importantly, Nrf2a attenuated age/disease-related dysfunction of Complex I and II supported  
604 coupled and uncoupled respiration and fatty acid oxidation in both sexes. Notably, Nrf2a  
605 selectively attenuated the age/disease-related decline in coupled respiration in males and  
606 uncoupled respiration in females. Nrf2a attenuated the age/disease-related declines in  
607 mitochondrial efficiency/coupling in males only. In humans, mitochondrial coupling decreases  
608 with age (Kumaran *et al.*, 2005). Exercise-induced attenuation in loss of mitochondrial  
609 efficiency/coupling with age (Conley *et al.*, 2013) has led researchers to speculate that  
610 improving mitochondrial efficiency may help attenuate sarcopenia (Harper *et al.*, 2021).  
611 Interestingly, in the presence of rotenone, a Complex I inhibitor, there was no effect of Nrf2a,  
612 which suggests that Nrf2a improves mitochondrial respiration through improvements in Complex  
613 I function. This is consistent with data from another study that used a different Nrf2 activator,  
614 sulforaphane, and demonstrated improvements in Complex I function (Bose *et al.*, 2020). The  
615 pathways underlying the effect of Nrf2 activation on mitochondrial function are not entirely  
616 understood. However, several studies have demonstrated that Nrf2 is a central mediator for  
617 improvements in mitochondrial function. Nrf2 at least partially mediates exercise-induced  
618 mitochondrial biogenesis and improvement in mitochondrial function (Merry & Ristow, 2016;  
619 D'Souza *et al.*, 2020; Islam *et al.*, 2020). Interestingly, both Nrf2-related redox signaling (Safdar  
620 *et al.*, 2010) and Complex I function decrease with age in skeletal muscle (Kruse *et al.*, 2016).  
621 Thus, Nrf2a may target a critical mechanism that contributes to age-related mitochondrial  
622 dysfunction, though the specific mechanisms by which Nrf2 activation might contribute to  
623 Complex I function remain to be elucidated.

625 As a master regulator of cytoprotective gene transcription, Nrf2 is a critical component of  
626 redox homeostasis. Skeletal muscle mitochondria of aged Nrf2 knock-out mice emit significantly  
627 more ROS than aged wildtype counterparts reflecting the role of Nrf2 in regulating redox  
628 balance (Kitaoka *et al.*, 2019). *In vitro*, Nrf2 knock out models have compromised Complex I  
629 activity due to impairments in NADH availability (Kovac *et al.*, 2015). Importantly, pyruvate  
630 dehydrogenase is a redox sensitive enzyme responsible for supplying NADH to Complex I  
631 (Fisher-Wellman *et al.*, 2015). Thus, age-related increases in oxidative stress may constrain the  
632 supply of NADH to Complex I, which would explain age-associated decline in Complex I  
633 capacity and how NAD<sup>+</sup> supplementation restores mitochondrial respiratory capacity (Kruse *et*  
634 *al.*, 2016; McElroy *et al.*, 2020). In our study, Nrf2a increased mitochondrial function, particularly

635 in Complex I, which may have been mediated by improved cellular redox regulation. However,  
636 future studies will need to more rigorously investigate the effect of Nrf2a on redox homeostasis.

637 Another potential mechanism by which Nrf2a enhanced mitochondrial function is through  
638 greater mitochondrial protein turnover. There was no consistent age- or treatment-related effect  
639 on mitochondrial protein content in the soleus or gastrocnemius (Supplemental Figure 7).  
640 However, there was an age/disease-related decline in mitochondrial biogenesis, suggesting  
641 that, in order to maintain mitochondrial density, degradation of mitochondrial proteins (i.e.  
642 mitophagy or ubiquitin dependent degradation of mitochondrial proteins) also declined. Impaired  
643 mitophagy contributes to mitochondrial dysfunction and disease in humans (Ryu *et al.*, 2016;  
644 Gouspillou *et al.*, 2018; Newman & Shadel, 2018). Importantly, Nrf2a attenuated the  
645 age/disease-related decline in mitochondrial protein synthesis, suggesting that declines in  
646 degradation/mitophagy may have also been attenuated, though we did not directly measure  
647 this. As such we posit that mitochondrial protein turnover, which is essential for maintenance of  
648 overall mitochondrial function (Szczepanowska & Trifunovic, 2021), was maintained in 15 mo  
649 Nrf2a guinea pigs compared to 15 mo CON guinea pigs in this study. Others have also  
650 demonstrated that Nrf2 activators play a role in modulating mitochondrial protein turnover. In *C.*  
651 *elegans* the Nrf2 homolog mediated Tomatidine-induced (a Nrf2 activator) mitophagy (Fang *et*  
652 *al.*, 2017). Our group has demonstrated that Protandim, also a phytochemical Nrf2 activator,  
653 enhanced mitochondrial protein turnover in wheel running rats (Bruns *et al.*, 2018). Thus, Nrf2  
654 activation seems to preserve mitochondrial protein turnover in 15 mo guinea pigs while turnover  
655 may have declined in 15 mo CON guinea pigs.

#### 656 *Nrf2a attenuates components of protein homeostasis*

657 Decline in mechanisms to maintain proteostasis (which includes not only protein  
658 synthesis and degradation, but also chaperone-mediated folding and protein trafficking (Noack  
659 *et al.*, 2014)) contributes to age-related musculoskeletal dysfunction (Kaushik & Cuervo, 2015;  
660 Santra *et al.*, 2019). There is limited insight on the effect of age on protein homeostasis in  
661 humans, though basal protein synthesis appears to be unchanged with age in humans (Volpi *et*  
662 *al.*, 2001; Brook *et al.*, 2016). Moreover, differences between men and women with regard to the  
663 decline in skeletal muscle proteostasis remains unclear. While men generally have greater  
664 muscle mass than women, men also lose muscle mass faster and muscle strength to a greater  
665 degree; however, women are less fatigue resistant (thoroughly reviewed in (Gheller *et al.*,  
666 2016). In the present study, we documented the age-related decline in protein synthesis in all  
667 subfractions of the soleus and gastrocnemius muscles of both male, which we observed in our  
668 previous study (Musi *et al.*, 2020), and female Hartley guinea pigs. There were no sex

669 differences in fractional synthesis rates in either muscle. This is the first study to characterize  
670 age-related declines in protein synthesis in female guinea pigs. It is important to note, however,  
671 that while we documented age-related differences in long-term protein synthesis rates to  
672 minimize the bias of faster turning over proteins (Miller *et al.*, 2015), it is possible that our  
673 approach may still not accurately determine differences in fractional synthesis rates between  
674 ages if the protein pools subject to turnover (i.e. the dynamic protein pools) are not the same  
675 between the 5 mo and 15 mo guinea pigs. As recently demonstrated by Abbott and Lawrence  
676 and colleagues, the dynamic protein pool declines with age and thus obscures the fractional  
677 synthesis rates and biases towards aged animals having lower synthesis rates (Abbott *et al.*,  
678 2021). The approach the authors employed is both novel and unique, but raises important  
679 considerations when evaluating the effect of age or interventions on protein turnover in the  
680 future. Employing such an approach may also help reconcile differences in observations on the  
681 effect of age on protein turnover between species (Volpi *et al.*, 2001; Miller *et al.*, 2019; Musci *et*  
682 *al.*, 2020) and more accurately describe the age-related effects on protein kinetics. Importantly,  
683 we agree with the authors that adopting such a rigorous approach in the future will provide  
684 better guidance as to how to improve proteome integrity and maintain the dynamic protein pool  
685 with age.

686 In the present study, Nrf2a attenuated the age/disease-related declines in myofibrillar  
687 and mitochondrial protein synthesis rates in the soleus in both males and females. Interestingly,  
688 Nrf2a had no attenuating effect on the age/disease-related declines of protein synthesis in any  
689 subfraction of the gastrocnemius. One driving factor of protein synthesis is cellular proliferation  
690 (Eden *et al.*, 2011). Thus, to discern protein synthesis dedicated to proliferation as opposed to  
691 proteome maintenance, we made simultaneous measurements of DNA synthesis rates to  
692 provide insight about the proportion of protein synthesis dedicated towards newly synthesized  
693 proteins compared to proteome maintenance (Miller *et al.*, 2014). There was no difference in the  
694 allocation of protein synthesis to proteome maintenance in the soleus or gastrocnemius in either  
695 male or female guinea pigs. Moreover, Nrf2a had no effect on protein carbonylation levels in  
696 either the soleus or gastrocnemius. These data are in contrast with our previous studies  
697 demonstrating that other Nrf2 activators promote proteome maintenance *in vitro* and *in vivo* in  
698 both rats (Bruns *et al.*, 2018) and humans (Konopka *et al.*, 2017). Importantly, interventions that  
699 activate mechanisms maintaining proteostasis are linked to healthspan extension in a variety of  
700 organisms (Pride *et al.*, 2015; Hamilton & Miller, 2017; Sands *et al.*, 2017). Thus, while Nrf2a  
701 attenuated the decline in protein synthesis in the present study, Nrf2a did not increase the  
702 proportion of proteins synthesized for proteome maintenance.

703        The mechanisms by which Nrf2a attenuated the decline in protein synthesis are not  
704 entirely clear. However, alleviating energetic constraints through enhanced mitochondrial  
705 function is a likely candidate to explain some of these improvements. Protein turnover is  
706 energetically demanding, accounting for nearly 35% of basal metabolism (Waterlow, 1984;  
707 Rolfe & Brown, 1997; Bier, 1999). Age-related impairments in mitochondrial function  
708 consequentially constrain the amount of energy dedicated to proteostasis. Mitochondrial  
709 dysfunction precedes the loss of proteostasis in skeletal muscle, which leads to declines in  
710 function (Ben-Zvi *et al.*, 2009; Gaffney *et al.*, 2018). Moreover, other interventions that attenuate  
711 the decline in or improve mitochondrial function, also improve proteostatic mechanisms and  
712 preserve overall muscle function. For example, maintaining physical activity and caloric  
713 restriction in rodents delays declines in mitochondrial function as well as skeletal muscle  
714 function (Zangarelli *et al.*, 2006; Stolle *et al.*, 2018), a similar observation made in masters  
715 athletes (Zampieri *et al.*, 2015). While both exercise and caloric restriction have broad effects,  
716 more targeted interventions focused on improving mitochondrial function also report a similar  
717 phenomenon: enhancing mitochondrial function delays skeletal muscle dysfunction (Gaffney *et*  
718 *al.*, 2018; Campbell *et al.*, 2019). This observation occurs in other tissues as well. Increasing  
719 mitochondrial proteostasis decreases proteotoxic amyloid aggregation in cells, increasing  
720 fitness and lifespan in *C. elegans* (Sorrentino *et al.*, 2017). These studies emphasize the  
721 importance of mitochondrial respiration and the production of ATP to facilitate proteostatic  
722 mechanisms. In humans, aerobic exercise improves mitochondrial function through  
723 mitochondrial remodeling and improves skeletal muscle function (Greggio *et al.*, 2017).  
724 Altogether, our data support the posit that Nrf2a-mediated improvements in mitochondrial  
725 respiration alleviated constraints in energy which led to greater amount of ATP available to  
726 support proteostasis.

727        Another mechanism by which Nrf2a may have attenuated declines in skeletal muscle  
728 proteostasis is through the mitigation of inflammation and oxidative stress, which can have  
729 deleterious effects on protein turnover, particularly protein synthesis. Protein synthesis, at rest,  
730 appears to be no different between young and old individuals (Volpi *et al.*, 2001; Brook *et al.*,  
731 2016). However, age-related inflammation and oxidative stress can blunt the anabolic response  
732 to stimuli such as exercise or feeding. This concept, termed anabolic resistance, is a contributor  
733 to age-related musculoskeletal dysfunction and appears to blunt the anabolic response to  
734 resistance exercise training (Cuthbertson *et al.*, 2005; Wilkes *et al.*, 2009; Burd *et al.*, 2012;  
735 Brook *et al.*, 2016). Interventions designed to mitigate age-related increases oxidative stress or  
736 inflammation seem to improve skeletal muscle anabolic responses to exercise (Trappe *et al.*,

737 2002), feeding (Rieu *et al.*, 2009; Smiles *et al.*, 2019), and insulin (Rivas *et al.*, 2016).  
738 Importantly, Nrf2a stimulates transcription of endogenous antioxidant and anti-inflammatory  
739 genes (Hybertson *et al.*, 2011; Hybertson *et al.*, 2019). Thus, it is possible that Nrf2a treatment  
740 ameliorated oxidative stress and inflammation and improved the anabolic response to feeding.  
741 However, because we measured cumulative protein synthesis over 30 days, rather than acutely  
742 in response to an anabolic stimulus such as feeding, we cannot determine if there were any  
743 changes specifically in the anabolic response to feeding. Future studies should investigate the  
744 efficacy of this particularly Nrf2a, PB125, on abrogating inflammation and oxidative stress and,  
745 in acute settings, determine whether Nrf2a enhances the anabolic response to feeding or  
746 activity. In the present study, there was no observed effect of treatment on ROS emission or  
747 protein oxidation. However, our lab has previously demonstrated that another Nrf2 activator  
748 increases antioxidant protein expression (Reuland *et al.*, 2013) and augmented protein  
749 synthesis related to proteostasis in skeletal muscle of rats in response to wheel running  
750 exercise (Bruns *et al.*, 2018). Thus, treatment with Nrf2 activators may represent a class of  
751 interventions that augment adaptation to acute stressors (Minci *et al.*, 2019).

#### 752 *Future Directions*

753 The improvements in mitochondrial respiration and proteostasis did not translate to  
754 sustained improvements in mobility. However, it is important to note that our measure of mobility  
755 is only one metric of musculoskeletal function. Additionally, musculoskeletal function is not the  
756 only factor that dictates mobility. Thus, it is still important to assess other and more specific  
757 components of musculoskeletal function, as mitochondrial function is a strong determinant in  
758 physical function such as gait speed and grip strength in humans (Gonzalez-Freire *et al.*, 2018).

759 Another observation that warrants further investigation are the sex-specific effects of  
760 Nrf2a. Other interventions involving Nrf2 activators have also demonstrated sex-specific effects.  
761 The Interventions Testing Program reported that treatment with the Nrf2 activator Protandim  
762 extended median lifespan in heterogenous male mice, but not females (Strong *et al.*, 2016). Our  
763 lab has also previously demonstrated that Protandim only improved myofibrillar proteostasis in  
764 men (Konopka *et al.*, 2017). Other healthspan promoting interventions, such as a metformin and  
765 rapamycin, also have sex specific effects (Strong *et al.*, 2016). We have begun interrogating  
766 these sex specific effects through the use of kinetic proteomics (Wolff *et al.*, 2019; Wolff *et al.*,  
767 2021). Moving forward, it will be necessary to interrogate these sex differences and the  
768 implications they have on the efficacy of Nrf2a to attenuate musculoskeletal decline. Females  
769 experience sarcopenia at a similar prevalence as males worldwide (Shafiee *et al.*, 2017), future  
770 investigation of targeting Nrf2 for musculoskeletal aging should include investigation of the

771 mechanisms likely to underlie our sex-specific responses including interaction of reproductive  
772 hormones with Nrf2 signaling.

773 **Conclusions**

774 Musculoskeletal dysfunction is a primary contributor to disability and dependence with  
775 age. There are few existing interventions that effectively mitigate the decline in skeletal muscle  
776 function with age. In this study, we further characterized a model for musculoskeletal  
777 dysfunction measuring mitochondrial function and protein synthesis in both male and female  
778 Hartley guinea pigs. Moreover, we tested a potential healthspan-extending phytochemical  
779 compound PB125, which is currently in the NIA-ITP  
780 (<https://www.nia.nih.gov/research/dab/interventions-testing-program-itp/compounds-testing>), on  
781 mitochondrial function and proteostasis in this pre-clinical guinea pig model of musculoskeletal  
782 decline. We found that this compound improved mitochondrial function and attenuated declines  
783 in protein synthesis, mechanisms that likely mediate improvements in function and longevity.  
784 This project adds to the growing literature that supports the use of Nrf2 activators to improve  
785 organismal health. The data from this study provide mechanistic insight by which a readily  
786 translatable intervention could mitigate age-related musculoskeletal decline.

787 **Acknowledgments**

788 We would like to thank Dr. Ann Hess of the Statistics Department at Colorado State University  
789 for overseeing and guiding the statistical analysis of this project. Pathways Bioscience provided  
790 the PB125 compound for this project. This work was funded by NIH grant R21 AG054713-02  
791 awarded to KLH and KSS and supported by the ACSM NASA Space Physiology Grant awarded  
792 to RVM.

793 **Author Contributions**

794 Study design: RVM, KMA, BFM, MAJ, JMM, BMH, KSS, KLH. Data collection: RVM, KMA,  
795 MAW, ZV, MFA, SB, MC, TJ, TEK, RM, TN, JS, SW, MDM, QZ. Data analysis: RVM, KMA,  
796 KSS, KLH. Manuscript preparation: RVM, KLH. All authors approved of the final manuscript.

797 **Role of Funding Source**

798 The funding sources had no impact on any aspect of the study.

799 **Conflict of Interest**

800 JMM and BMH are members of the R&D team at the company that produces PB125. Neither  
801 JMM or BMH were responsible for data collection or analysis. No other authors have conflicts of  
802 interest to disclose.

803

804 Abbott CB, Lawrence MM, Kobak KA, Lopes EBP, Peelor FF, Donald EJ, Van Remmen H, Griffin  
805 TM & Miller BF. (2021). A Novel Stable Isotope Approach Demonstrates Surprising  
806 Degree of Age-Related Decline in Skeletal Muscle Collagen Proteostasis. *Function* **2**,  
807 Ahead of Print.

808

809 Ahmed SM, Luo L, Namani A, Wang XJ & Tang X. (2017). Nrf2 signaling pathway: Pivotal roles in  
810 inflammation. *Biochim Biophys Acta Mol Basis Dis* **1863**, 585-597.

811

812 Atella V, Piano Mortari A, Kopinska J, Belotti F, Lapi F, Cricelli C & Fontana L. (2019). Trends in  
813 age-related disease burden and healthcare utilization. *Aging Cell* **18**, e12861.

814

815 Bakula D, Ablasser A, Aguzzi A, Antebi A, Barzilai N, Bittner MI, Jensen MB, Calkhoven CF, Chen  
816 D, Grey A, Feige JN, Georgievskaya A, Gladyshev VN, Golato T, Gudkov AV, Hoppe T,  
817 Kaeberlein M, Katajisto P, Kennedy BK, Lal U, Martin-Villalba A, Moskalev AA, Ozerov I,  
818 Petr MA, Reason, Rubinsztein DC, Tyshkovskiy A, Vanhaelen Q, Zhavoronkov A &  
819 Scheibye-Knudsen M. (2019). Latest advances in aging research and drug discovery.  
820 *Aging (Albany NY)* **11**, 9971-9981.

821

822 Baskin KK, Winders BR & Olson EN. (2015). Muscle as a "mediator" of systemic metabolism. *Cell  
823 Metab* **21**, 237-248.

824

825 Ben-Zvi A, Miller EA & Morimoto RI. (2009). Collapse of proteostasis represents an early  
826 molecular event in *Caenorhabditis elegans* aging. *Proc Natl Acad Sci U S A* **106**, 14914-  
827 14919.

828

829 Bier DM. (1999). *The Role of Protein and Amino Acids in Sustaining and Enhancing Performance*.  
830 National Academies Press.

831

832 Bonewald LF, Kiel DP, Clemens TL, Esser K, Orwoll ES, O'Keefe RJ & Fielding RA. (2013). Forum  
833 on bone and skeletal muscle interactions: summary of the proceedings of an ASBMR  
834 workshop. *J Bone Miner Res* **28**, 1857-1865.

835

836 Bose C, Alves I, Singh P, Palade PT, Carvalho E, Børshøj E, Jun S-R, Cheema A, Boerma M,  
837 Awasthi S & Singh SP. (2020). Sulforaphane prevents age-associated cardiac and  
838 muscular dysfunction through Nrf2 signaling. *Aging Cell*, e13261.

839

840 Brook MS, Wilkinson DJ, Mitchell WK, Lund JN, Phillips BE, Szewczyk NJ, Greenhaff PL, Smith K &  
841 Atherton PJ. (2016). Synchronous deficits in cumulative muscle protein synthesis and  
842 ribosomal biogenesis underlie age-related anabolic resistance to exercise in humans. *J  
843 Physiol* **594**, 7399-7417.

844

845 Bruns DR, Ehrlicher SE, Khademi S, Biela LM, Peelor FF, 3rd, Miller BF & Hamilton KL. (2018).  
846 Differential effects of vitamin C or protandim on skeletal muscle adaptation to exercise.  
847 *J Appl Physiol* **125**, 661-671.

848

849 Burd NA, Wall BT & Loon LJCv. (2012). The curious case of anabolic resistance: old wives' tales  
850 or new fables? *J Appl Physiol* **112**, 1233-1235.

851

852 Busch R, Kim Y-K, Neese RA, Schade-Serin V, Collins M, Awada M, Gardner JL, Beysen C, Marino  
853 ME, Misell LM & Hellerstein MK. (2005). Measurement of protein turnover rates by  
854 heavy water labeling of nonessential amino acids. *Biochimica Et Biophysica Acta Bba -*  
855 *Gen Subj* **1760**, 730-744.

856

857 Busch R, Neese RA, Awada M, Hayes GM & Hellerstein MK. (2007). Measurement of cell  
858 proliferation by heavy water labeling. *Nat Protoc* **2**, 3045-3057.

859

860 Campbell MD, Duan J, Samuelson AT, Gaffrey MJ, Merrihew GE, Egertson JD, Wang L, Bammler  
861 TK, Moore RJ, White CC, Kavanagh TJ, Voss JG, Szeto HH, Rabinovitch PS, MacCoss MJ,  
862 Qian WJ & Marcinek DJ. (2019). Improving mitochondrial function with SS-31 reverses  
863 age-related redox stress and improves exercise tolerance in aged mice. *Free Radic Biol  
864 Med* **134**, 268-281.

865

866 Cardinale DA, Larsen FJ, Schiffer TA, Morales-Alamo D, Ekblom B, Calbet JAL, Holmberg HC &  
867 Boushel R. (2018). Superior Intrinsic Mitochondrial Respiration in Women Than in Men.  
868 *Front Physiol* **9**, 1133.

869

870 Collins JA, Diekman BO & Loeser RF. (2018). Targeting aging for disease modification in  
871 osteoarthritis. *Curr Opin Rheumatol* **30**, 101-107.

872

873 Collins JA, Wood ST, Nelson KJ, Rowe MA, Carlson CS, Chubinskaya S, Poole LB, Furdui CM &  
874 Loeser RF. (2016). Oxidative Stress Promotes Peroxiredoxin Hyperoxidation and  
875 Attenuates Pro-survival Signaling in Aging Chondrocytes. *J Biol Chem* **291**, 6641-6654.

876

877 Conley KE, Jubrias SA, Cress ME & Esselman PC. (2013). Elevated energy coupling and aerobic  
878 capacity improves exercise performance in endurance-trained elderly subjects. *Exp  
879 Physiol* **98**, 899-907.

880

881 Cuthbertson D, Smith K, Babraj J, Leese G, Waddell T, Atherton P, Wackerhage H, Taylor PM &  
882 Rennie MJ. (2005). Anabolic signaling deficits underlie amino acid resistance of wasting,  
883 aging muscle. *FASEB J* **19**, 422-424.

884

885 D'Souza RF, Woodhead JST, Hedges CP, Zeng NN, Wan JX, Kumagai H, Lee C, Cohen P, Cameron-  
886 Smith D, Mitchell CJ & Merry TL. (2020). Increased expression of the mitochondrial  
887 derived peptide, MOTS-c, in skeletal muscle of healthy aging men is associated with  
888 myofiber composition. *Aging-US* **12**, 5244-5258.

889  
890 DiGirolamo DJ, Kiel DP & Esser KA. (2013). Bone and skeletal muscle: neighbors with close ties. *J  
891 Bone Miner Res* **28**, 1509-1518.

892  
893 Distefano G, Standley RA, Dube JJ, Carnero EA, Ritov VB, Stefanovic-Racic M, Toledo FG, Piva SR,  
894 Goodpaster BH & Coen PM. (2017). Chronological Age Does not Influence Ex-vivo  
895 Mitochondrial Respiration and Quality Control in Skeletal Muscle. *J Gerontol A Biol Sci  
896 Med Sci* **72**, 535-542.

897  
898 Donovan EL, McCord JM, Reuland DJ, Miller BF & Hamilton KL. (2012). Phytochemical activation  
899 of Nrf2 protects human coronary artery endothelial cells against an oxidative challenge.  
900 *Oxid Med Cell Longev* **2012**, 132931.

901  
902 Drake JC, Bruns DR, Peelor FF, 3rd, Biela LM, Miller RA, Miller BF & Hamilton KL. (2015). Long-  
903 lived Snell dwarf mice display increased proteostatic mechanisms that are not  
904 dependent on decreased mTORC1 activity. *Aging Cell* **14**, 474-482.

905  
906 Drake JC, Bruns DR, Peelor FF, Biela LM, Miller RA, Hamilton KL & Miller BF. (2014). Long-lived  
907 crowded-litter mice have an age-dependent increase in protein synthesis to DNA  
908 synthesis ratio and mTORC1 substrate phosphorylation. *Am J Physiol-endoc M* **307**,  
909 E813-E821.

910  
911 Drake JC, Peelor FF, 3rd, Biela LM, Watkins MK, Miller RA, Hamilton KL & Miller BF. (2013).  
912 Assessment of mitochondrial biogenesis and mTORC1 signaling during chronic  
913 rapamycin feeding in male and female mice. *J Gerontol A Biol Sci Med Sci* **68**, 1493-1501.

914  
915 Eden E, Geva-Zatorsky N, Issaeva I, Cohen A, Dekel E, Danon T, Cohen L, Mayo A & Alon U.  
916 (2011). Proteome half-life dynamics in living human cells. *Science* **331**, 764-768.

917  
918 Fang EF, Waltz TB, Kassahun H, Lu QP, Kerr JS, Morevati M, Fivenson EM, Wollman BN, Marosi  
919 K, Wilson MA, Iser WB, Eckley DM, Zhang YQ, Lehrmann E, Goldberg IG, Scheibye-  
920 Knudsen M, Mattson MP, Nilsen H, Bohr VA & Becker KG. (2017). Tomatidine enhances  
921 lifespan and healthspan in C-elegans through mitophagy induction via the SKN-1/Nrf2  
922 pathway. *Sci Rep* **7**, 46208.

923  
924 Farnaghi S, Prasadam I, Cai G, Friis T, Du Z, Crawford R, Mao X & Xiao Y. (2017). Protective  
925 effects of mitochondria-targeted antioxidants and statins on cholesterolinduced  
926 osteoarthritis. *FASEB J* **31**, 356-367.

927  
928 Fisher-Wellman KH, Lin CT, Ryan TE, Reese LR, Gilliam LA, Cathey BL, Lark DS, Smith CD, Muoio  
929 DM & Neufer PD. (2015). Pyruvate dehydrogenase complex and nicotinamide nucleotide  
930 transhydrogenase constitute an energy-consuming redox circuit. *Biochem J* **467**, 271-  
931 280.

932

933 Gaffney CJ, Pollard A, Barratt TF, Constantin-Teodosiu D, Greenhaff PL & Szewczyk NJ. (2018).  
934       Greater loss of mitochondrial function with ageing is associated with earlier onset of  
935       sarcopenia in *C. elegans*. *Aging* **10**, 1-15.

936

937 Gao L, Kumar V, Vellichirammal NN, Park SY, Rudebush TL, Yu L, Son WM, Pekas EJ, Wafi AM,  
938       Hong J, Xiao P, Guda C, Wang HJ, Schultz HD & Zucker IH. (2020). Functional, proteomic  
939       and bioinformatic analyses of Nrf2- and Keap1- null skeletal muscle. *J Physiol* **598**, 5427-  
940       5451.

941

942 García-Hermoso A, Cavero-Redondo I, Ramírez-Vélez R, Ruiz J, Ortega FB, Lee D-C & Martínez-  
943       Vizcaíno V. (2018). Muscular strength as a predictor of all-cause mortality in apparently  
944       healthy population: a systematic review and meta-analysis of data from approximately 2  
945       million men and women. *Arch Phys Med Rehab* **99**, 2100-2113.e2105.

946

947 Gheller BJF, Riddle ES, Lem MR & Thalacker-Mercer AE. (2016). Understanding Age-Related  
948       Changes in Skeletal Muscle Metabolism: Differences Between Females and Males. *Annu  
949       Rev Nutr, Vol 36* **36**, 129-156.

950

951 Goates S, Du K, Arensberg MB, Gaillard T, Guralnik J & Pereira SL. (2019). Economic Impact of  
952       Hospitalizations in US Adults with Sarcopenia. *J Frailty Aging* **8**, 93-99.

953

954 Goldman DP, Cutler D, Rowe JW, Michaud PC, Sullivan J, Peneva D & Olshansky SJ. (2013).  
955       Substantial health and economic returns from delayed aging may warrant a new focus  
956       for medical research. *Health Aff (Millwood)* **32**, 1698-1705.

957

958 Gonzalez-Freire M, de Cabo R, Bernier M, Sollott SJ, Fabbri E, Navas P & Ferrucci L. (2015).  
959       Reconsidering the Role of Mitochondria in Aging. *J Gerontol A Biol Sci Med Sci* **70**, 1334-  
960       1342.

961

962 Gonzalez-Freire M, Scalzo P, D'Agostino J, Moore ZA, Diaz-Ruiz A, Fabbri E, Zane A, Chen B,  
963       Becker KG, Lehrmann E, Zukley L, Chia CW, Tanaka T, Coen PM, Bernier M, de Cabo R &  
964       Ferrucci L. (2018). Skeletal muscle ex vivo mitochondrial respiration parallels decline in  
965       vivo oxidative capacity, cardiorespiratory fitness, and muscle strength: The Baltimore  
966       Longitudinal Study of Aging. *Aging Cell* **17**.

967

968 Gorbunova V, Bozzella MJ & Seluanov A. (2008). Rodents for comparative aging studies: from  
969       mice to beavers. *Age (Dordr)* **30**, 111-119.

970

971 Gouspillou G, Godin R, Piquereau J, Picard M, Mofarrahi M, Mathew J, Purves-Smith FM,  
972       Sgarioto N, Hepple RT, Burelle Y & Hussain SNA. (2018). Protective role of Parkin in  
973       skeletal muscle contractile and mitochondrial function. *J Physiol* **596**, 2565-2579.

974

975 Greggio C, Jha P, Kulkarni SS, Lagarrigue S, Broskey NT, Boutant M, Wang X, Conde Alonso S,  
976 Ofori E, Auwerx J, Canto C & Amati F. (2017). Enhanced Respiratory Chain Supercomplex  
977 Formation in Response to Exercise in Human Skeletal Muscle. *Cell Metab* **25**, 301-311.  
978  
979 Groennebaek T, Jespersen NR, Jakobsgaard JE, Sieljacks P, Wang J, Rindom E, Musci RV, Botker  
980 HE, Hamilton KL, Miller BF, de Paoli FV & Vissing K. (2018). Skeletal Muscle  
981 Mitochondrial Protein Synthesis and Respiration Increase With Low-Load Blood Flow  
982 Restricted as Well as High-Load Resistance Training. *Front Physiol* **9**, 1796.  
983  
984 Hall BK. (2012). *Cartilage V1: Structure, Function, and Biochemistry*. Elsevier Science.  
985  
986 Hamilton KL & Miller BF. (2017). Mitochondrial proteostasis as a shared characteristic of slowed  
987 aging: the importance of considering cell proliferation. *J Physiol* **595**, 6401-6407.  
988  
989 Harper C, Gopalan V & Goh J. (2021). Exercise rescues mitochondrial coupling in aged skeletal  
990 muscle: a comparison of different modalities in preventing sarcopenia. *J Transl Med* **19**,  
991 71.  
992  
993 Houghton CA, Fassett RG & Coombes JS. (2016). Sulforaphane and Other Nutrigenomic Nrf2  
994 Activators: Can the Clinician's Expectation Be Matched by the Reality? *Oxid Med Cell  
995 Longev* **2016**, 7857186.  
996  
997 Hybertson BM, Gao B, Bose S & McCord JM. (2019). Phytochemical Combination PB125  
998 Activates the Nrf2 Pathway and Induces Cellular Protection against Oxidative Injury.  
999 *Antioxidants (Basel)* **8**, 119.  
1000  
1001 Hybertson BM, Gao B, Bose SK & McCord JM. (2011). Oxidative stress in health and disease: the  
1002 therapeutic potential of Nrf2 activation. *Mol Aspects Med* **32**, 234-246.  
1003  
1004 Islam H, Bonafiglia JT, Turnbull PC, Simpson CA, Perry CGR & Gurd BJ. (2020). The impact of  
1005 acute and chronic exercise on Nrf2 expression in relation to markers of mitochondrial  
1006 biogenesis in human skeletal muscle. *Eur J Appl Physiol* **120**, 149-160.  
1007  
1008 Jacques M, Kuang J, Bishop DJ, Yan X, Alvarez-Romero J, Munson F, Garnham A, Papadimitriou I,  
1009 Voisin S & Eynon N. (2020). Mitochondrial respiration variability and simulations in  
1010 human skeletal muscle: The Gene SMART study. *FASEB J* **34**, 2978-2986.  
1011  
1012 Jimenez PA, Glasson SS, Trubetskoy OV & Haimes HB. (1997). Spontaneous osteoarthritis in  
1013 Dunkin Hartley guinea pigs: histologic, radiologic, and biochemical changes. *Lab Anim Sci*  
1014 **47**, 598-601.  
1015  
1016 Kaeberlein M, Rabinovitch PS & Martin GM. (2015). Healthy aging: The ultimate preventative  
1017 medicine. *Science* **350**, 1191-1193.  
1018

1019 Karakelides H, Irving BA, Short KR, O'Brien P & Nair KS. (2010). Age, obesity, and sex effects on  
1020 insulin sensitivity and skeletal muscle mitochondrial function. *Diabetes* **59**, 89-97.

1021

1022 Kaushik S & Cuervo AM. (2015). Proteostasis and aging. *Nat Med* **21**, 1406-1415.

1023

1024 Kemmler W, Teschler M, Goisser S, Bebenek M, von Stengel S, Bollheimer LC, Sieber CC &  
1025 Freiberger E. (2015). Prevalence of sarcopenia in Germany and the corresponding effect  
1026 of osteoarthritis in females 70 years and older living in the community: results of the  
1027 FORMoSA study. *Clin Interv Aging* **10**, 1565-1573.

1028

1029 Kennedy BK, Berger SL, Brunet A, Campisi J, Cuervo AM, Epel ES, Franceschi C, Lithgow GJ,  
1030 Morimoto RI, Pessin JE, Rando TA, Richardson A, Schadt EE, Wyss-Coray T & Sierra F.  
1031 (2014). Geroscience: linking aging to chronic disease. *Cell* **159**, 709-713.

1032

1033 Kent-Braun JA & Ng AV. (2000). Skeletal muscle oxidative capacity in young and older women  
1034 and men. *J Appl Physiol* **89**, 1072-1078.

1035

1036 Kitaoka Y, Tamura Y, Takahashi K, Takeda K, Takemasa T & Hatta H. (2019). Effects of Nrf2  
1037 deficiency on mitochondrial oxidative stress in aged skeletal muscle. *Physiol Rep* **7**,  
1038 e13998.

1039

1040 Kobayashi EH, Suzuki T, Funayama R, Nagashima T, Hayashi M, Sekine H, Tanaka N, Moriguchi T,  
1041 Motohashi H, Nakayama K & Yamamoto M. (2016). Nrf2 suppresses macrophage  
1042 inflammatory response by blocking proinflammatory cytokine transcription. *Nat  
1043 Commun* **7**, 11624.

1044

1045 Kobayashi M & Yamamoto M. (2006). Nrf2-Keap1 regulation of cellular defense mechanisms  
1046 against electrophiles and reactive oxygen species. *Adv Enzyme Regul* **46**, 113-140.

1047

1048 Konopka AR, Asante A, Lanza IR, Robinson MM, Johnson ML, Dalla Man C, Cobelli C, Amols MH,  
1049 Irving BA & Nair KS. (2015). Defects in mitochondrial efficiency and H<sub>2</sub>O<sub>2</sub> emissions in  
1050 obese women are restored to a lean phenotype with aerobic exercise training. *Diabetes*  
1051 **64**, 2104-2115.

1052

1053 Konopka AR, Laurin JL, Musci RV, Wolff CA, Reid JJ, Biela LM, Zhang Q, Peelor FF, 3rd, Melby CL,  
1054 Hamilton KL & Miller BF. (2017). Influence of Nrf2 activators on subcellular skeletal  
1055 muscle protein and DNA synthesis rates after 6 weeks of milk protein feeding in older  
1056 adults. *Geroscience* **39**, 175-186.

1057

1058 Kovac S, Angelova PR, Holmstrom KM, Zhang Y, Dinkova-Kostova AT & Abramov AY. (2015).  
1059 Nrf2 regulates ROS production by mitochondria and NADPH oxidase. *Biochim Biophys  
1060 Acta* **1850**, 794-801.

1061

1062 Kruse SE, Karunadharma PP, Basisty N, Johnson R, Beyer RP, MacCoss MJ, Rabinovitch PS &  
1063 Marcinek DJ. (2016). Age modifies respiratory complex I and protein homeostasis in a  
1064 muscle type-specific manner. *Aging Cell* **15**, 89-99.

1065

1066 Kubo E, Chhunchha B, Singh P, Sasaki H & Singh DP. (2017). Sulforaphane reactivates cellular  
1067 antioxidant defense by inducing Nrf2/ARE/Prdx6 activity during aging and oxidative  
1068 stress. *Sci Rep* **7**, 14130.

1069

1070 Kumaran S, Panneerselvam KS, Shila S, Sivarajan K & Panneerselvam C. (2005). Age-associated  
1071 deficit of mitochondrial oxidative phosphorylation in skeletal muscle: role of carnitine  
1072 and lipoic acid. *Mol Cell Biochem* **280**, 83-89.

1073

1074 Lee SY, Ro HJ, Chung SG, Kang SH, Seo KM & Kim DK. (2016). Low Skeletal Muscle Mass in the  
1075 Lower Limbs Is Independently Associated to Knee Osteoarthritis. *Plos One* **11**, e0166385  
1076 0166311.

1077

1078 Loeser RF. (2010). Age-related changes in the musculoskeletal system and the development of  
1079 osteoarthritis. *Clin Geriatr Med* **26**, 371-386.

1080

1081 Lopez-Otin C, Blasco MA, Partridge L, Serrano M & Kroemer G. (2013). The hallmarks of aging.  
1082 *Cell* **153**, 1194-1217.

1083

1084 McElroy GS, Reczek CR, Reyfman PA, Mithal DS, Horbinski CM & Chandel NS. (2020). NAD+  
1085 Regeneration Rescues Lifespan, but Not Ataxia, in a Mouse Model of Brain  
1086 Mitochondrial Complex I Dysfunction. *Cell Metab* **32**, 301-308.e306.

1087

1088 Merry TL & Ristow M. (2016). Nuclear factor erythroid-derived 2-like 2 (NFE2L2, Nrf2) mediates  
1089 exercise-induced mitochondrial biogenesis and the anti-oxidant response in mice. *J  
1090 Physiol* **594**, 5195-5207.

1091

1092 Miller BF, Baehr LM, Musci RV, Reid JJ, Peelor FF, 3rd, Hamilton KL & Bodine SC. (2019). Muscle-  
1093 specific changes in protein synthesis with aging and reloading after disuse atrophy. *J  
1094 Cachexia Sarcopenia Muscle* **10**, 1195-1209.

1095

1096 Miller BF, Drake JC, Naylor B, Price JC & Hamilton KL. (2014). The measurement of protein  
1097 synthesis for assessing proteostasis in studies of slowed aging. *Ageing Res Rev* **18**, 106-  
1098 111.

1099

1100 Miller BF, Konopka AR & Hamilton KL. (2016). The rigorous study of exercise adaptations: why  
1101 mRNA might not be enough. *J Appl Physiology* **121**, 594-596.

1102

1103 Miller BF, Reid JJ, Price JC, Lin H-JL, Atherton PJ & Smith K. (2020). Cores of Reproducibility in  
1104 Physiology: The Use of Deuterated Water for the Measurement of Protein Synthesis. *J  
1105 Appl Physiology*.

1106  
1107 Miller BF, Robinson MM, Bruss MD, Hellerstein M & Hamilton KL. (2012). A comprehensive  
1108 assessment of mitochondrial protein synthesis and cellular proliferation with age and  
1109 caloric restriction. *Aging Cell* **11**, 150-161.  
1110  
1111 Miller BF, Robinson MM, Reuland DJ, Drake JC, Peelor FF, 3rd, Bruss MD, Hellerstein MK &  
1112 Hamilton KL. (2013). Calorie restriction does not increase short-term or long-term  
1113 protein synthesis. *J Gerontol A Biol Sci Med Sci* **68**, 530-538.  
1114  
1115 Miller BF, Wolff CA, Peelor FF, 3rd, Shipman PD & Hamilton KL. (2015). Modeling the  
1116 contribution of individual proteins to mixed skeletal muscle protein synthetic rates over  
1117 increasing periods of label incorporation. *J Appl Physiol* **118**, 655-661.  
1118  
1119 Miotto PM, McGlory C, Holloway TM, Phillips SM & Holloway GP. (2018). Sex differences in  
1120 mitochondrial respiratory function in human skeletal muscle. *Am J Physiol Regul Integr  
1121 Comp Physiol* **314**, R909-R915.  
1122  
1123 Musci RV, Hamilton KL & Linden MA. (2019). Exercise-Induced Mitohormesis for the  
1124 Maintenance of Skeletal Muscle and Healthspan Extension. *Sports (Basel)* **7**, 170 118.  
1125  
1126 Musci RV, Hamilton KL & Miller BF. (2018). Targeting mitochondrial function and proteostasis to  
1127 mitigate dynapenia. *Eur J Appl Physiol* **118**, 1-9.  
1128  
1129 Musci RV, Walsh MA, Konopka AR, Wolff CA, Peelor FF, 3rd, Reiser RF, 2nd, Santangelo KS &  
1130 Hamilton KL. (2020). The Dunkin Hartley Guinea Pig Is a Model of Primary Osteoarthritis  
1131 That Also Exhibits Early Onset Myofiber Remodeling That Resembles Human  
1132 Musculoskeletal Aging. *Front Physiol* **11**, 571372.  
1133  
1134 Newman LE & Shadel GS. (2018). Pink1/Parkin link inflammation, mitochondrial stress, and  
1135 neurodegeneration. *J Cell Biol* **217**, 3327-3329.  
1136  
1137 Noack J, Brambilla Pisoni G & Molinari M. (2014). Proteostasis: bad news and good news from  
1138 the endoplasmic reticulum. *Swiss Med Wkly* **144**, w14001.  
1139  
1140 Noehren B, Kosmac K, Walton RG, Murach KA, Lyles MF, Loeser RF, Peterson CA & Messier SP.  
1141 (2018). Alterations in quadriceps muscle cellular and molecular properties in adults with  
1142 moderate knee osteoarthritis. *Osteoarthritis Cartilage* **26**, 1359-1368.  
1143  
1144 Ogawa Y, Kaneko Y, Sato T, Shimizu S, Kanetaka H & Hanyu H. (2018). Sarcopenia and Muscle  
1145 Functions at Various Stages of Alzheimer Disease. *Front Neurol* **9**, 710.  
1146  
1147 Pesta D & Gnaiger E. (2011). High-Resolution Respirometry: OXPHOS Protocols for Human Cells  
1148 and Permeabilized Fibers from Small Biopsies of Human Muscle. *Methods Mol Biology*  
1149 *Clifton NJ* **810**, 25-58.

1150  
1151 Piantadosi CA, Carraway MS, Babiker A & Suliman HB. (2008). Heme oxygenase-1 regulates  
1152 cardiac mitochondrial biogenesis via Nrf2-mediated transcriptional control of nuclear  
1153 respiratory factor-1. *Circ Res* **103**, 1232-1240.  
1154  
1155 Pride H, Yu Z, Sunchu B, Mochnick J, Coles A, Zhang Y, Buffenstein R, Hornsby PJ, Austad SN &  
1156 Perez VI. (2015). Long-lived species have improved proteostasis compared to  
1157 phylogenetically-related shorter-lived species. *Biochem Biophys Res Commun* **457**, 669-  
1158 675.  
1159  
1160 Quesenberry KF, Orcutt CJ, Mans C & Carpenter JW. (2021). *Ferrets, Rabbits, and Rodents*  
1161 *Clinical Medicine and Surgery*.  
1162  
1163 Relaix F, Bencze M, Borok MJ, Der Vartanian A, Gattazzo F, Mademtzoglou D, Perez-Diaz S, Prola  
1164 A, Reyes-Fernandez PC, Rotini A & Taglietti t. (2021). Perspectives on skeletal muscle  
1165 stem cells. *Nat Commun* **12**, 692.  
1166  
1167 Reuland DJ, Khademi S, Castle CJ, Irwin DC, McCord JM, Miller BF & Hamilton KL. (2013).  
1168 Upregulation of phase II enzymes through phytochemical activation of Nrf2 protects  
1169 cardiomyocytes against oxidant stress. *Free Radic Biol Med* **56**, 102-111.  
1170  
1171 Rieu I, Magne H, Savary-Azeloux I, Averous J, Bos C, Peyron MA, Combaret L & Dardevet D.  
1172 (2009). Reduction of low grade inflammation restores blunting of postprandial muscle  
1173 anabolism and limits sarcopenia in old rats. *J Physiol* **587**, 5483-5492.  
1174  
1175 Rivas DA, McDonald DJ, Rice NP, Haran PH, Dolnikowski GG & Fielding RA. (2016). Diminished  
1176 anabolic signaling response to insulin induced by intramuscular lipid accumulation is  
1177 associated with inflammation in aging but not obesity. *Am J Physiol Regul Integr Comp*  
1178 *Physiol* **310**, R561 569.  
1179  
1180 Robinson MM, Turner SM, Hellerstein MK, Hamilton KL & Miller BF. (2011). Long-term synthesis  
1181 rates of skeletal muscle DNA and protein are higher during aerobic training in older  
1182 humans than in sedentary young subjects but are not altered by protein  
1183 supplementation. *FASEB J* **25**, 3240-3249.  
1184  
1185 Rolfe DF & Brown GC. (1997). Cellular energy utilization and molecular origin of standard  
1186 metabolic rate in mammals. *Physiol Rev* **77**, 731-758.  
1187  
1188 Roux CH, Guillemin F, Boini S, Longuetaud F, Arnault N, Hercberg S & Briancon S. (2005). Impact  
1189 of musculoskeletal disorders on quality of life: an inception cohort study. *Ann Rheum Dis*  
1190 **64**, 606-611.  
1191  
1192 Ryu D, Mouchiroud L, Andreux PA, Katsyuba E, Moullan N, Nicolet-Dit-Felix AA, Williams EG, Jha  
1193 P, Lo Sasso G, Huzard D, Aebischer P, Sandi C, Rinsch C & Auwerx J. (2016). Urolithin A

1194        induces mitophagy and prolongs lifespan in *C. elegans* and increases muscle function in  
1195        rodents. *Nat Med* **22**, 879-888.

1196

1197        Sands WA, Page MM & Selman C. (2017). Proteostasis and ageing: insights from long-lived  
1198        mutant mice. *J Physiol* **595**, 6383-6390.

1199

1200        Santangelo KS, Kaeding AC, Baker SA & Bertone AL. (2014). Quantitative Gait Analysis Detects  
1201        Significant Differences in Movement between Osteoarthritic and Nonosteoarthritic  
1202        Guinea Pig Strains before and after Treatment with Flunixin Meglumine. *Arthritis* **2014**,  
1203        503519-503518.

1204

1205        Santangelo KS, Pieczarka EM, Nuovo GJ, Weisbrode SE & Bertone AL. (2011). Temporal  
1206        expression and tissue distribution of interleukin-1beta in two strains of guinea pigs with  
1207        varying propensity for spontaneous knee osteoarthritis. *Osteoarthritis Cartilage* **19**, 439-  
1208        448.

1209

1210        Santra M, Dill KA & de Graff AMR. (2019). Proteostasis collapse is a driver of cell aging and  
1211        death. *Proc Natl Acad Sci U S A* **116**, 22173-22178.

1212

1213        Shafiee G, Keshtkar A, Soltani A, Ahadi Z, Larijani B & Heshmat R. (2017). Prevalence of  
1214        sarcopenia in the world: a systematic review and meta- analysis of general population  
1215        studies. *J Diabetes Metab Disord* **16**, 21.

1216

1217        Short KR, Bigelow ML, Kahl J, Singh R, Coenen-Schimke J, Raghavakaimal S & Nair KS. (2005).  
1218        Decline in skeletal muscle mitochondrial function with aging in humans. *Proc Natl Acad  
1219        Sci U S A* **102**, 5618-5623.

1220

1221        Sieljacks P, Wang J, Groennebaek T, Rindom E, Jakobsgaard JE, Herskind J, Gravholt A, Moller  
1222        AB, Musci RV, de Paoli FV, Hamilton KL, Miller BF & Vissing K. (2019). Six Weeks of Low-  
1223        Load Blood Flow Restricted and High-Load Resistance Exercise Training Produce Similar  
1224        Increases in Cumulative Myofibrillar Protein Synthesis and Ribosomal Biogenesis in  
1225        Healthy Males. *Front Physiol* **10**, 649.

1226

1227        Smiles WJ, Churchward-Venne TA, van Loon LJC, Hawley JA & Camera DM. (2019). A single bout  
1228        of strenuous exercise overcomes lipid-induced anabolic resistance to protein ingestion  
1229        in overweight, middle-aged men. *FASEB J* **33**, 7009-7017.

1230

1231        Sorrentino V, Romani M, Mouchiroud L, Beck JS, Zhang H, D'Amico D, Moullan N, Potenza F,  
1232        Schmid AW, Rietsch S, Counts SE & Auwerx J. (2017). Enhancing mitochondrial  
1233        proteostasis reduces amyloid-beta proteotoxicity. *Nature* **552**, 187-193.

1234

1235        Stolle S, Ciapaite J, Reijne AC, Talarovicova A, Wolters JC, Aguirre-Gamboa R, van der Vlies P, de  
1236        Lange K, Neerincx PB, van der Vries G, Deelen P, Swertz MA, Li Y, Bischoff R, Permentier  
1237        HP, Horvatovitch PL, Groen AK, van Dijk G, Reijngoud DJ & Bakker BM. (2018). Running-

1238 wheel activity delays mitochondrial respiratory flux decline in aging mouse muscle via a  
1239 post-transcriptional mechanism. *Aging Cell* **17**, e12700-12711.

1240

1241 Strong R, Miller RA, Antebi A, Astle CM, Bogue M, Denzel MS, Fernandez E, Flurkey K, Hamilton  
1242 KL, Lamming DW, Javors MA, de Magalhaes JP, Martinez PA, McCord JM, Miller BF,  
1243 Muller M, Nelson JF, Nduku J, Rainger GE, Richardson A, Sabatini DM, Salmon AB,  
1244 Simpkins JW, Steegenga WT, Nadon NL & Harrison DE. (2016). Longer lifespan in male  
1245 mice treated with a weakly estrogenic agonist, an antioxidant, an alpha-glucosidase  
1246 inhibitor or a Nrf2-inducer. *Aging Cell* **15**, 872-884.

1247

1248 Szczepanowska K & Trifunovic A. (2021). Tune instead of destroy: How proteolysis keeps  
1249 OXPHOS in shape. *Biochim Biophys Acta Bioenerg* **1862**, 148365.

1250

1251 Tonge DP, Bardsley RG, Parr T, Maciewicz RA & Jones SW. (2013). Evidence of changes to  
1252 skeletal muscle contractile properties during the initiation of disease in the ageing  
1253 guinea pig model of osteoarthritis. *Longev Healthspan* **2**, 15.

1254

1255 Trappe TA, White F, Lambert CP, Cesar D, Hellerstein M & Evans WJ. (2002). Effect of ibuprofen  
1256 and acetaminophen on postexercise muscle protein synthesis. *Am J Physiol Endocrinol  
1257 Metab* **282**, E551-556.

1258

1259 United States Bone and Joint Initiative (2020). The Burden of Musculoskeletal Diseases in the  
1260 United States (BMUS). 4<sup>th</sup> edn.

1261

1262 Vaananen HK. (1993). Mechanism of bone turnover. *Ann Med* **25**, 353-359.

1263

1264 Volpi E, Sheffield-Moore M, Rasmussen BB & Wolfe RR. (2001). Basal muscle amino acid kinetics  
1265 and protein synthesis in healthy young and older men. *JAMA* **286**, 1206-1212.

1266

1267 Walston J, Hadley EC, Ferrucci L, Guralnik JM, Newman AB, Studenski SA, Ershler WB, Harris T &  
1268 Fried LP. (2006). Research agenda for frailty in older adults: toward a better  
1269 understanding of physiology and etiology: summary from the American Geriatrics  
1270 Society/National Institute on Aging Research Conference on Frailty in Older Adults. *J Am  
1271 Geriatr Soc* **54**, 991-1001.

1272

1273 Waterlow JC. (1984). Protein turnover with special reference to man. *Q J Exp Physiol* **69**, 409-  
1274 438.

1275

1276 Wilkes EA, Selby AL, Atherton PJ, Patel R, Rankin D, Smith K & Rennie MJ. (2009). Blunting of  
1277 insulin inhibition of proteolysis in legs of older subjects may contribute to age-related  
1278 sarcopenia. *Am J Clin Nutr* **90**, 1343-1350.

1279

1280 Williams GR, Deal AM, Muss HB, Weinberg MS, Sanoff HK, Guerard EJ, Nyrop KA, Pergolotti M &  
1281 Shachar SS. (2018). Frailty and skeletal muscle in older adults with cancer. *J Geriatr  
1282 Oncol* **9**, 68-73.

1283

1284 Wolff CA, Lawrence MM, Porter H, Zhang Q, Reid JJ, Laurin JL, Musci RV, Linden MA, Peelor FF,  
1285 3rd, Wren JD, Creery JS, Cutler KJ, Carson RH, Price JC, Hamilton KL & Miller BF. (2021).  
1286 Sex differences in changes of protein synthesis with rapamycin treatment are minimized  
1287 when metformin is added to rapamycin. *Geroscience* **43**, 809-828.

1288

1289 Wolff CA, Reid JJ, Musci RV, Linden MA, Konopka AR, Peelor FF, Miller BF & Hamilton KL. (2019).  
1290 Differential Effects of Rapamycin and Metformin in Combination with Rapamycin on  
1291 Mechanisms of Proteostasis in Cultured Skeletal Myotubes. *J Gerontol A Biol Sci Med Sci*  
1292 **128**, 412.

1293

1294 Yoshimura Y, Wakabayashi H, Yamada M, Kim H, Harada A & Arai H. (2017). Interventions for  
1295 Treating Sarcopenia: A Systematic Review and Meta-Analysis of Randomized Controlled  
1296 Studies. *J Am Med Dir Assoc* **18**, 553 e551-553 e516.

1297

1298 Zampieri S, Pietrangelo L, Loefler S, Fruhmann H, Vogelauer M, Burggraf S, Pond A, Grim-Stieger  
1299 M, Cvecka J, Sedliak M, Tirpakova V, Mayr W, Sarabon N, Rossini K, Barberi L, De Rossi  
1300 M, Romanello V, Boncompagni S, Musaro A, Sandri M, Protasi F, Carraro U & Kern H.  
1301 (2015). Lifelong physical exercise delays age-associated skeletal muscle decline. *J  
1302 Gerontol A Biol Sci Med Sci* **70**, 163-173.

1303

1304 Zangarelli A, Chanseaume E, Morio B, Brugere C, Mosoni L, Rousset P, Giraudet C, Patrac V,  
1305 Gachon P, Boirie Y & Walrand S. (2006). Synergistic effects of caloric restriction with  
1306 maintained protein intake on skeletal muscle performance in 21-month-old rats: a  
1307 mitochondria-mediated pathway. *FASEB J* **20**, 2439-2450.

1308

1309

1310

1311 **Figure 1** Study Design. There were two cohorts of guinea pigs in this study. The first cohort was  
1312 treated with Nrf2a or vehicle control from 2 mo to 5 mo, during which knee OA begins  
1313 developing. The second cohort was treated from 5 mo to 15 mo of age, after which knee OA  
1314 begins developing and during which detectable declines in musculoskeletal quality arise. In the  
1315 final 30 days of each study, a bolus I.P. injection of  $^2\text{H}_2\text{O}$  was administered and  $^2\text{H}_2\text{O}$  was mixed  
1316 in drinking for measurement of protein synthesis. A portion of the soleus was harvested for  
1317 mitochondrial respirometry assessments. Another portion of the soleus as well as a portion of  
1318 the gastrocnemius was harvested for isotopic measurements. Comparisons between 5 mo and  
1319 15 mo guinea pigs were made between the cohorts at the day of harvest. Longitudinal weight  
1320 and mobility data were acquired from the second cohort.

1321 **Figure 2** Age-, Sex-, and Treatment-related differences in mitochondrial respiration. There was  
1322 a significant negative effect of Age on State 3<sub>[CI-CIV]</sub> respiration ( $p=0.001$ ). Female guinea pigs  
1323 had lower levels of respiration compared to males ( $p=0.006$ ). Treatment did not significantly  
1324 increase respiration ( $p=0.098$ ) **(A)**. Electron transport system capacity (ETS<sub>[CI-CIV]</sub>) significantly  
1325 decreased with age ( $p=0.004$ ) and was lower in females ( $p=0.002$ ). Nrf2a treatment increased  
1326 respiration ( $p=0.037$ ). The interaction effect between Sex and Age was insignificant ( $p=0.058$ )  
1327 **(B)**. There was a significant decrease in Complex II – IV uncoupled respiration with age  
1328 ( $p<0.0001$ ), but there was no effect of Treatment. Female guinea pigs had lower respiration  
1329 compared to male guinea pigs ( $p=0.002$  effect of Sex) **(C)**. Mitochondrial efficiency (RCR)  
1330 decreased with age ( $p=0.012$ ) **(D)**.

1331 **Figure 3** Fatty acid supported respiration. There was no difference in fatty acid supported  
1332 respiration with 0.5 mM ADP between Sex, Age, or Treatment groups **(A)**. Fatty acid supported  
1333 respiration with 1.0 mM was lower in females ( $p=0.029$  effect of Sex), but the effect of  
1334 Treatment was insignificant ( $p=0.086$ ) **(B)**. At saturating amounts of ADP (6.0 mM), female  
1335 guinea pigs had lower fatty acid supported respiration compared ( $p=0.030$  effect of Sex), though  
1336 there was not a significant difference between 5 mo and 15 mo guinea pigs ( $p=0.058$  effect of  
1337 Age). Nrf2a treatment did not have a significant effect on respiration ( $p=0.098$ ) **(C)**.

1338 **Figure 4** Nrf2a treatment improves ADP Vmax. There was an age-related increase in ADP  
1339 Vmax ( $p=0.049$ ), though female guinea pigs had a lower Vmax compared males ( $p=0.001$ ).  
1340 Nrf2a significant increased ADP Vmax ( $p=0.026$ ). Post-hoc analysis revealed Nrf2a 5 mo  
1341 female had greater ADP Vmax compared to CON 5 mo female guinea pigs ( $p=0.045$ ) **(A)**. There  
1342 was a significant increase in ADP Km from Nrf2a treatment ( $p=0.007$ ). There was an  
1343 insignificant interaction between Sex and Treatment ( $p=0.092$ ) **(B)**.

1344 **Figure 5** Nrf2a attenuates age-related declines in mitochondrial respiration. There was no  
1345 difference in ADP Vmax between 5mo and 15mo CON guinea pigs ( $p=0.109$ ), whereas 15mo  
1346 Nrf2a guinea pigs had a higher ADP Vmax than 5mo CON guinea pigs ( $p=0.072$ ) (**A**).  
1347 Comparing sex-specific effects, Nrf2a only had a positive effect in male guinea pigs only  
1348 ( $p=0.021$ ) (**B**). There was an age-related decrease ( $p=0.024$ ) in State 3<sub>[PGM + S]</sub> between CON  
1349 guinea pigs, though this difference was attenuated in 15mo Nrf2a guinea pigs ( $p=0.536$ ) (**C**).  
1350 The age-related decline though, was only observed in female guinea pigs ( $p=0.046$ ), which was  
1351 attenuated by Nrf2a ( $p=0.290$ ) (**D**). Uncoupled respiration ETS<sub>[C<sub>I</sub> – C<sub>IV</sub>]</sub> non-significantly ( $p=0.061$ )  
1352 decreased with age, though Nrf2a attenuated this difference ( $p=0.875$ ) (**E**), though there were  
1353 no significant differences when sex was considered (**F**). There was a significant decrease  
1354 ( $p<0.0001$ ) in ETS<sub>[C<sub>II</sub> – C<sub>IV</sub>]</sub> between 5 mo and 15 mo CON guinea pigs that Nrf2a did not  
1355 attenuate ( $p=0.0006$ ) (**G**) in either sex (**H**).

1356 **Figure 6** Fractional synthesis rates (FSR) of both the soleus and gastrocnemius subfractions  
1357 decrease with age. FSR significantly decreased with age in all subfractions of the soleus  
1358 ( $p=0.002$ ,  $p=0.003$ ,  $p<0.0001$ ,  $p<0.0001$  for myofibrillar (**A**), mitochondrial (**B**), cytosolic (**C**), and  
1359 collagen (**D**) subfractions, respectively). 15 mo guinea pigs also had a significant decrease in  
1360 FSR in every subfraction of gastrocnemius as well ( $p<0.0001$  for all subfractions) (**E – H**).

1361 **Figure 7** Nrf2a treatment attenuates age-related declines in FSR of soleus subfractions. 15 mo  
1362 CON guinea pigs had lower FSR in each subfraction of the soleus ( $p=0.0021$ ,  $p=0.030$ ,  
1363  $p<0.0001$ ,  $p<0.0001$  for the myofibrillar (**A**), mitochondrial (**C**), cytosolic (**E**), and collagen (**G**)  
1364 subfractions, respectively). Nrf2a attenuated the decline in the myofibrillar (**A**) and mitochondrial  
1365 (**C**) subfractions, but not in the cytosolic (**E**) or collagen subfractions (**G**). Nrf2a attenuated the  
1366 decline in myofibrillar FSR in both males ( $p=0.920$ ) and females ( $p=0.166$ ) (**B**) and attenuated  
1367 the decline in cytosolic FSR in males only ( $p=0.207$ ) (**F**).

1368 **Figure 8** Nrf2a treatment does not attenuate the age-related decline in FSR in the  
1369 gastrocnemius. 15 mo CON guinea pigs had significantly lower FSR compared to 5 mo CON  
1370 guinea pigs in each subfraction ( $p<0.0001$  for all subfractions) (**A, C, E, G**). The FSR of all  
1371 subfractions of the gastrocnemius in 15 mo Nrf2a guinea pigs were also significantly lower  
1372 compared to 5 mo CON guinea pigs ( $p<0.0001$  for all subfractions) (**A, C, E, G**). This pattern  
1373 was observed in both male and female guinea pigs (**B, D, F, H**).

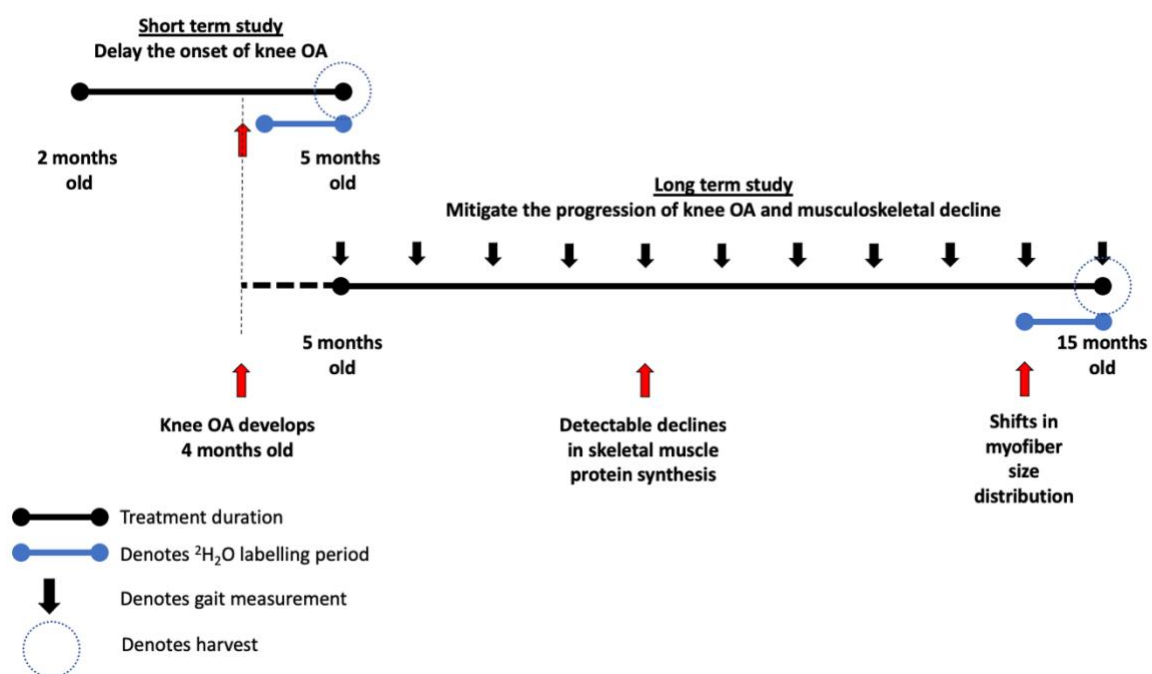
1374 **Figure 9** The effect of Nrf2a treatment on PRO:DNA synthesis ratios in the soleus and  
1375 gastrocnemius. There was no effect of Nrf2a treatment in the myofibrillar, mitochondrial, or  
1376 cytosolic subfractions on the ratio of protein to DNA synthesis in either the soleus or  
1377 gastrocnemius of 15 mo male or female guinea pigs.

1378 **Figure 10** The probability of maintained mobility. There was a greater proportion of Nrf2a  
1379 treated male (**A**) and female (**B**) guinea pigs that maintained mobility over the course of the  
1380 study period. However, there was no statistically significant effect of Nrf2a on the probability of  
1381 maintaining mobility throughout the course of the study.

1382

1383 **Figure 1**

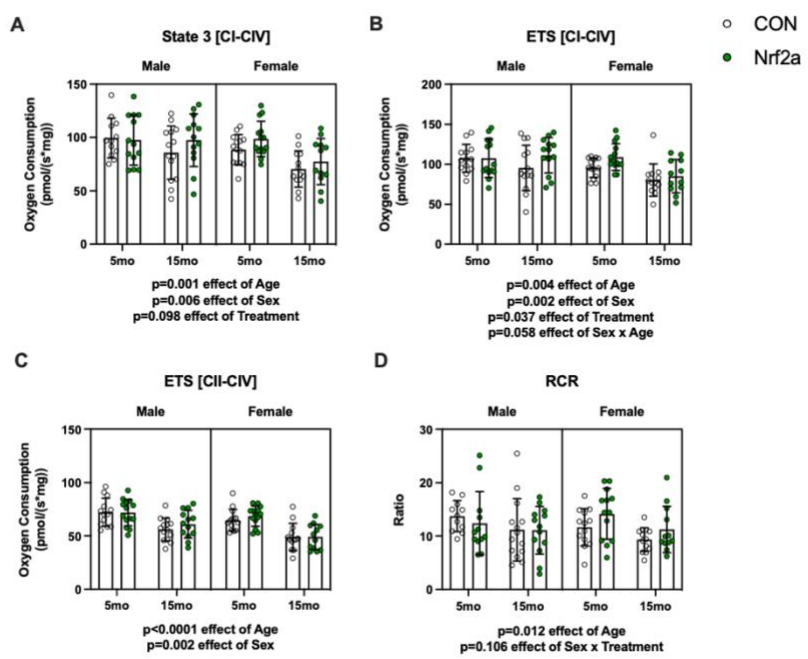
1384



1385

1386

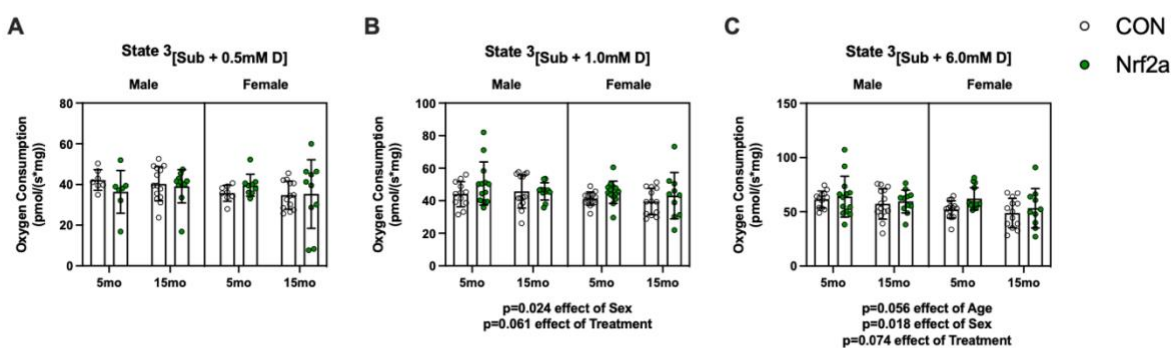
1387 **Figure 2**



1388

1389

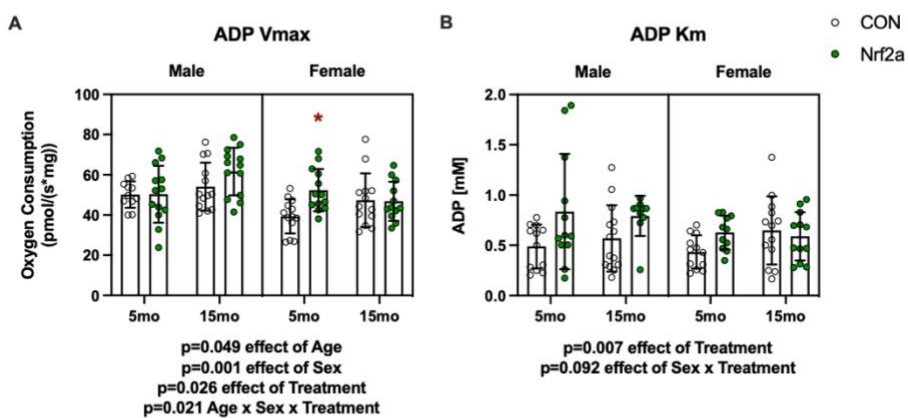
1390 **Figure 3**



1391

1392

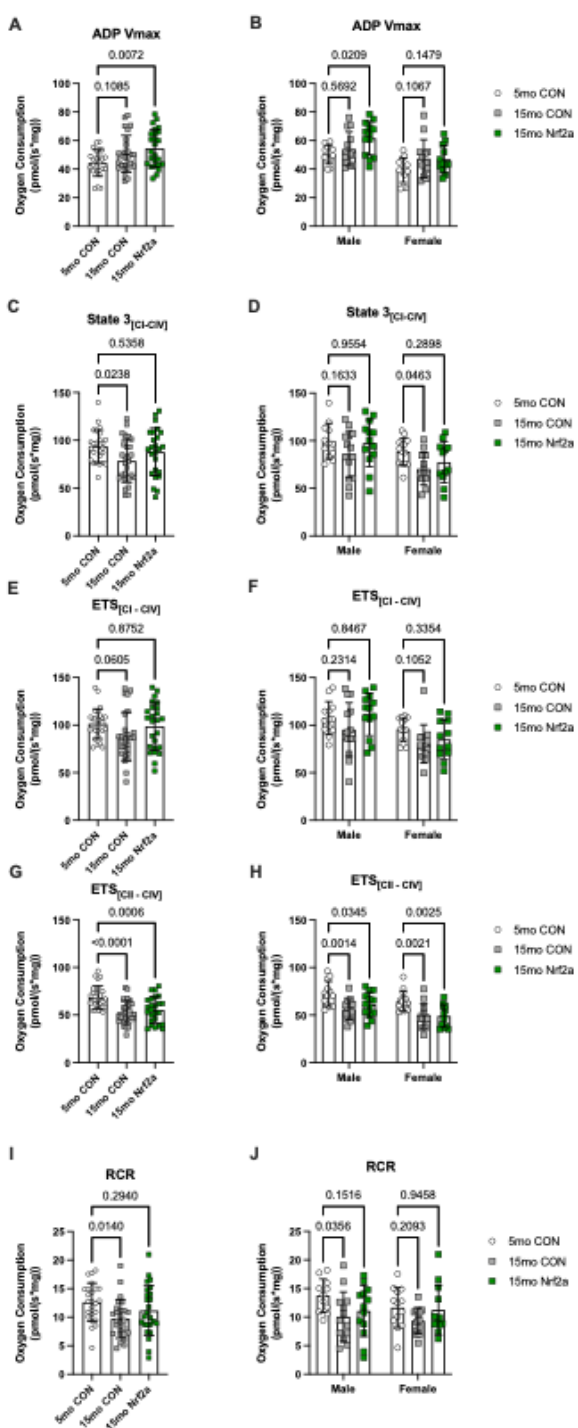
1393 **Figure 4**



1394

1395

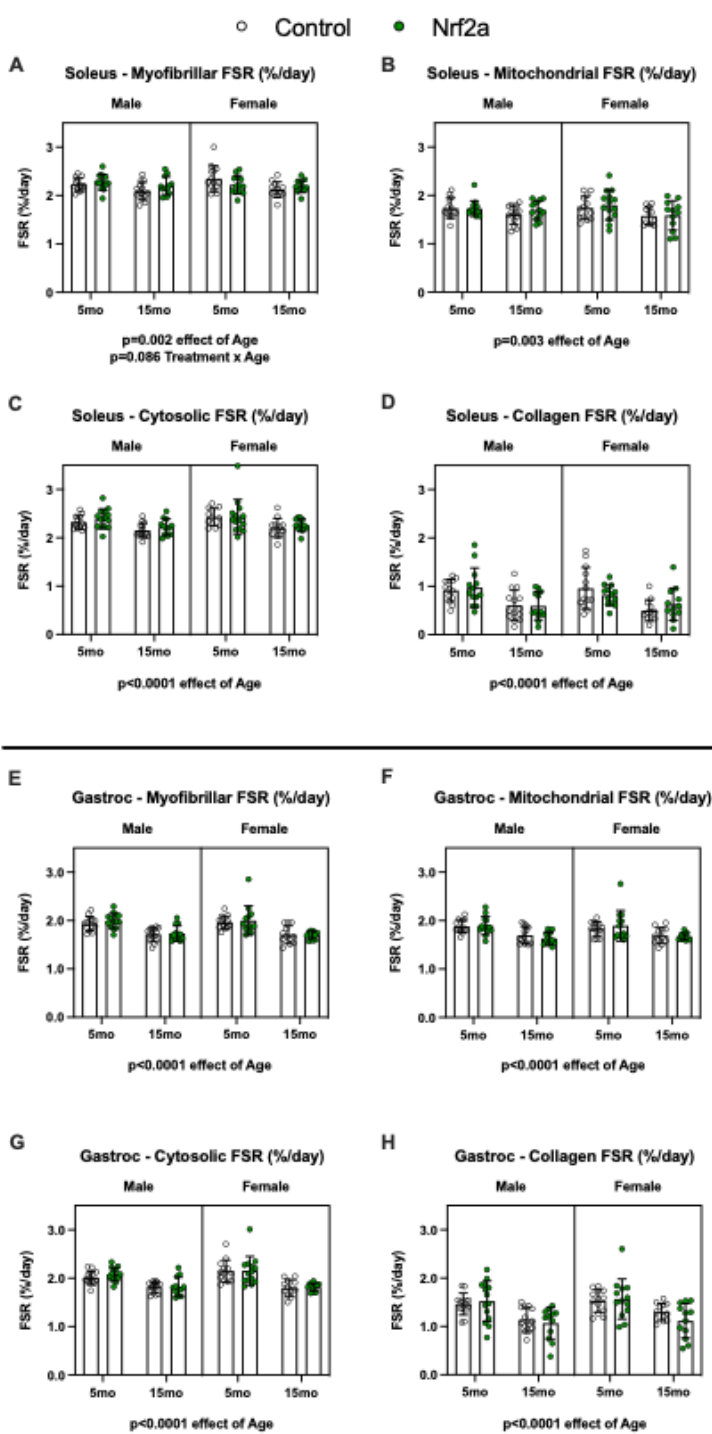
1396 **Figure 5**



1397

1398

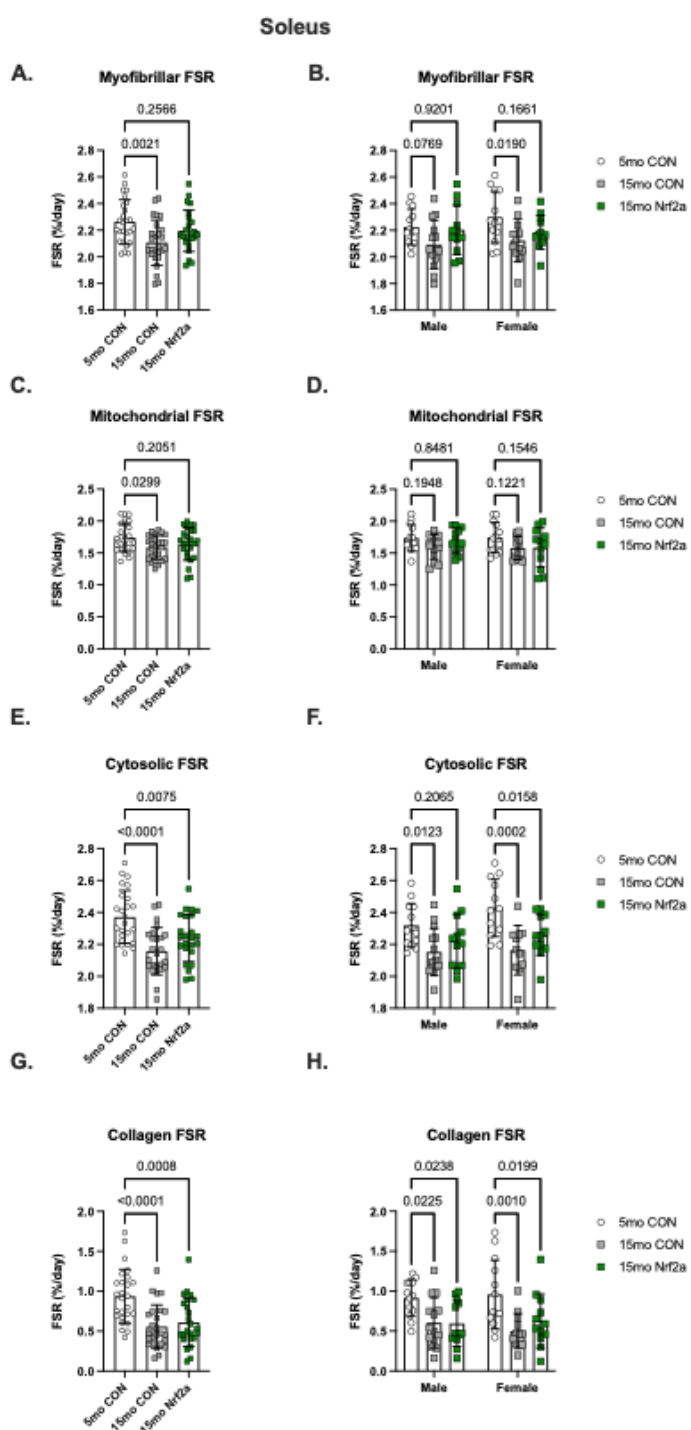
1399 **Figure 6**



1400

1401

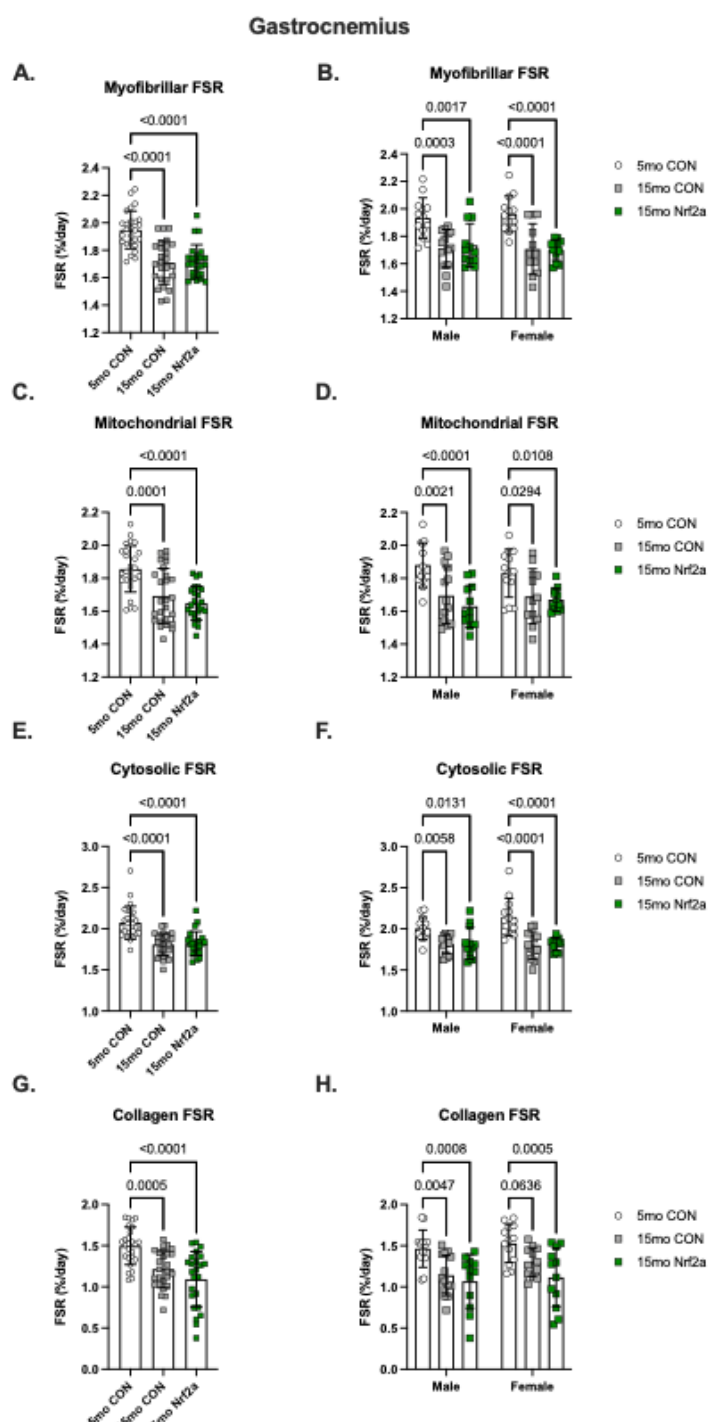
1402 **Figure 7**



1403

1404

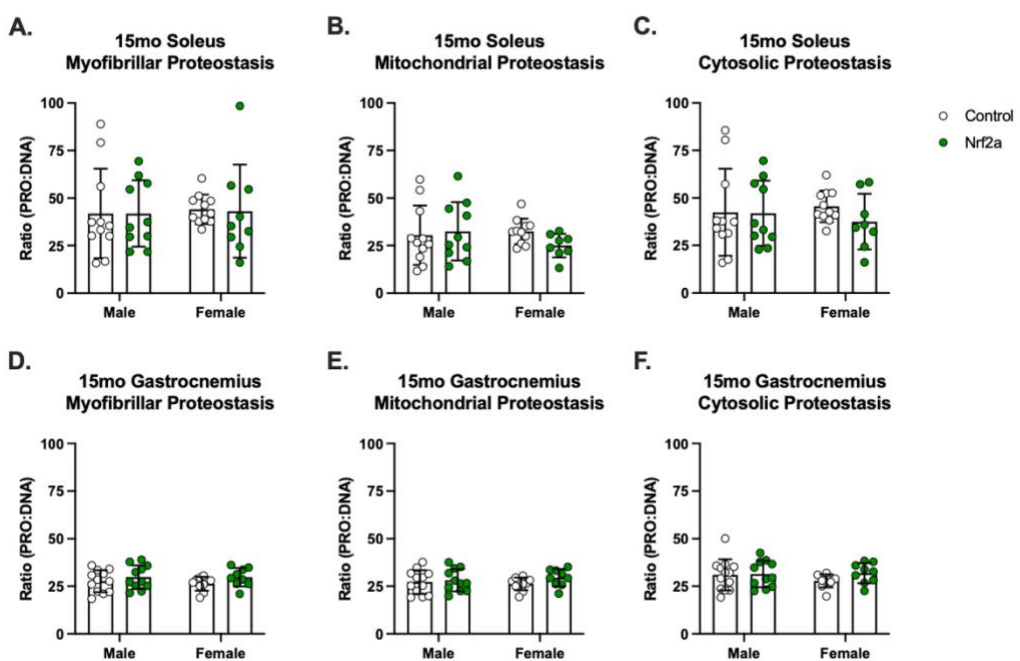
1405 **Figure 8**



1406

1407

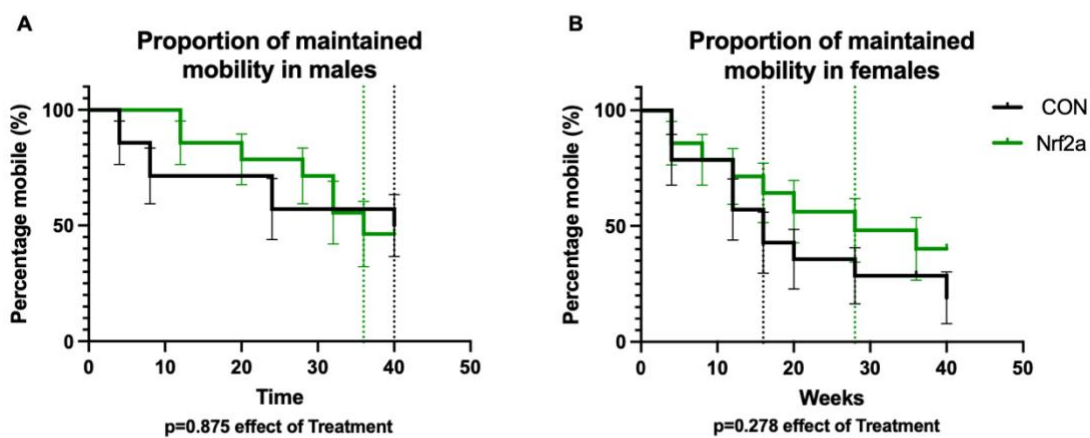
1408 **Figure 9**



1409

1410

1411 **Figure 10**



1412

1413